

# Rate of epidemic spreading on complex networks

Samuel Cure, Florian G. Pflug, and Simone Pigolotti\*

*Biological Complexity Unit, Okinawa Institute of Science and Technology, Onna, Okinawa 904-0495, Japan.*

(Dated: August 6, 2024)

The initial phase of an epidemic is often characterized by an exponential increase in the number of infected individuals. In this Letter, we predict the exponential spreading rate of an epidemic on a complex network. We first find an expression of the reproduction number for a network, based on the degree distribution, the network assortativity, and the level of clustering. We then connect this reproduction number and the disease infectiousness to the spreading rate. Our result holds for a broad range of networks, apart from networks with very broad degree distribution, where no clear exponential regime is present. Our theory bridges the gap between classic epidemiology and the theory of complex network, with broad implications for model inference and policy making.

Epidemic modeling permits rationalization of evidences and provides crucial information for policy making. Epidemiological models should incorporate the key features that determine epidemic spreading. For example, social structures play a crucial role in epidemic spreading [1], and in the effectiveness of intervention strategies [2, 3]. In these social structures, the number of contacts per individual is highly variable. For instance, individuals with most contacts contributed disproportionately to the spreading of COVID-19 [4, 5].

Social structures can be conveniently modeled by means of complex networks [6], in which nodes represent individuals and links denote pairs of individuals that are in contact. A success of network theory has been to determine the epidemic threshold on networks [7–9], i.e., the transition point from a localized outbreak to a widespread epidemic. This theory has shown that scale-free networks are extremely vulnerable to epidemics [7, 9–11]. Clustering, i.e., the tendency of nodes to form tightly connected communities, also affects epidemic spreading. Many real-world networks possess both heavy-tailed degree distribution and high level of clustering [12].

Another key feature of an epidemic is its infectiousness, i.e., the rate at which an infected individual infects its contacts. The infectiousness incorporates multiple factors, such as the viral load, social behavior, and possibly environmental factors [13]. Because of changes in these factors, the infectiousness of an individual changes over time in a way that is particular to each disease. This time-dependence profoundly impacts how a disease spreads.

Social structures and individual infectiousness are crucial in determining the initial stage of an epidemic, in which most individuals are susceptible and the number of infected individuals usually grows exponentially. This stage is of central importance for novel epidemics, or during emergence of novel variants, as it often requires rapid policy making. At later stages, other factors become relevant, such as individual recovery time, their behavioral response [14], and the possible occurrence of reinfections.

Despite the vast body of theory on epidemics in net-

works [9], general results on the speed of epidemic spreading are surprisingly sparse. The rate of epidemic spreading can be calculated for unclustered, uncorrelated networks, and with constant infectiousness [15]. A recent theory estimates the average time it takes for an epidemic to reach an individual at a certain distance from patient zero [16]. The spread of an epidemic on a network can be exactly solved [17], but this calculation is practically feasible only for very small networks. Other approaches avoid a detailed description of social structures, and effectively model the population heterogeneity by assigning different risk propensities to individuals [18, 19].

In this Letter, we theoretically predict the exponential rate of epidemic spreading on a complex network. Our theory quantifies the impact of main properties of the network, such as assortativity and clustering, on the reproduction number of the epidemic. We further link the reproduction number and the individual infectiousness with the exponential spreading rate. Our approach leads to precise predictions for a broad range of networks.

*Epidemic spreading in well-mixed populations.* We begin by summarizing how the exponential spreading rate of an epidemic is determined in well-mixed populations [13]. In this case, the cumulative number  $I(t)$  of infected individuals at time  $t$  is governed by the renewal equation

$$\dot{I}(t) = R_0 \int_0^t d\tau w(\tau) \dot{I}(t - \tau), \quad (1)$$

where the basic reproduction number  $R_0$  represents the average number of secondary infections by each infected individual, and the dot denotes a time derivative. The function  $w(\tau)$  represents the probability density that a given secondary infection occurs after a time  $\tau$  from the primary one. Equation (1) is linear because of the assumption that the epidemic is in the exponential stage and thus far from saturation. We now substitute the ansatz  $I(t) \sim e^{\Lambda t}$  into Eq. (1) and take the limit of large  $t$ , obtaining the Euler-Lotka equation

$$\frac{1}{R_0} = \langle e^{-\Lambda \tau} \rangle, \quad (2)$$

where the average  $\langle \dots \rangle$  is over the distribution  $w(\tau)$ .

Equation (2) is a cornerstone in mathematical epidemiology, as it provides a fundamental link between the three key quantities governing the epidemic spreading: the distribution of infection times  $w(\tau)$ ; the basic reproduction number  $R_0$ ; and the exponential spreading rate  $\Lambda$ .

*Epidemic spreading on networks.* We now consider a structured population composed of  $N$  individuals, who are represented as nodes on a network (Fig. 1a). Two individuals are connected by a link if they are in contact, meaning that they can potentially infect one another. An infected individual spreads the disease to each of its neighbors with rate  $\lambda(\tau)$ , where  $\tau$  is the time since the individual was infected. The probability that the individual infects a given neighbor at time  $\tau$ , given that the neighbor has not been infected before by someone else, is then equal to  $\psi(\tau) = \lambda(\tau) \exp[-\int_0^\tau \lambda(\tau') d\tau']$ . We call  $\psi(\tau)$  the generation time distribution (Fig. 1b). The integral  $p_\psi = \int_0^\tau \psi(\tau') d\tau'$  represents the total probability of infecting a susceptible neighbor. Aside from this normalization, the generation time distribution plays the role of  $w(\tau)$  for networks. In the following, we focus for simplicity on the case  $p_\psi = 1$ , where individuals infect all of their contacts and the epidemic eventually spreads through all the network, if the network is connected. Our results can be extended to the case  $p_\psi < 1$  by randomly removing links in the networks, see [20].

Over the course of the epidemic, each individual can be infected at most once and never formally recovers, although their infectiousness may wane over time. Our model can thus be seen as a non-Markovian Susceptible-Infected model. The time dependence of  $\lambda(\tau)$  is important to model real-world epidemics. For example, the infectiousness of COVID-19 markedly increases for 3–6 days and then decays for about 11 days [21], and is therefore poorly described by a Markovian model with constant  $\lambda(\tau)$ .

In the model, the number of infected individuals grows in time until it saturates (Fig. 1c). An alternative to the temporal perspective is to represent the epidemic in generations (Fig. 1d). We call  $Z_n$ ,  $n = 0, 1, \dots$  the average number of infected individuals in the  $n$ th generation. The initial generation,  $n = 0$ , is constituted by the patient zero,  $Z_0 = 1$ . In this representation, the infected individuals form a tree (Fig. 1e).

*Reproduction number on a network.* The basic reproduction number  $R_0$  for a network is the average number of links of an infected individual in the early stage of the epidemic, excluding the one from whom the infection came from. The effective reproduction number  $R$  is the average number of infections caused by an infected individual. In contrast with  $R_0$ ,  $R$  does not include contacts that are infected by other individuals. This difference is crucial in clustered networks.

To estimate  $R$  for a network, we characterize individuals by their degree  $k$ . We introduce the reproduction

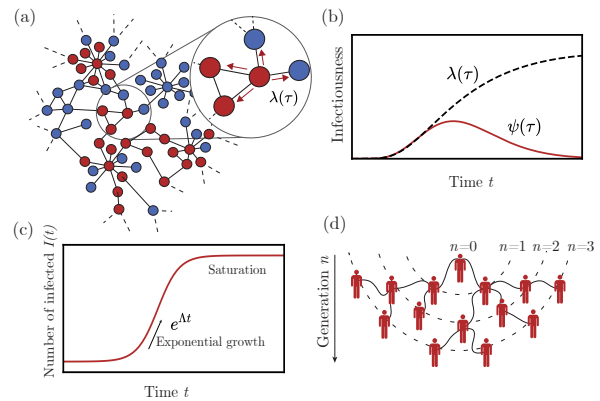


FIG. 1. (a) Epidemic spreading on a network. Individuals (nodes) can be infected (red) or healthy (blue). Infected individuals spread the infection at a rate  $\lambda(\tau)$  to each of their neighbors, where  $\tau$  is the time since they were infected. If neighbors have already been infected, transmission does not result in an infection. (b) Time-dependent spreading rate  $\lambda(\tau)$  and resulting distribution  $\psi(\tau)$  of infection times. (c) An epidemic trajectory. The exponential phase ends in a saturation phase, where a sizeable fraction of the individuals are infected. (d) Epidemic tree. The epidemic initiates with one infected individual (patient zero). Subsequent infections are represented by continuous lines. Dashed lines represent generations.

matrix

$$M_{kk'} = (k' - 1 - m_{kk'})P(k|k'), \quad (3)$$

whose elements are the average numbers of susceptible individuals of degree  $k$  connected to a node of degree  $k'$ . In Eq. (3),  $P(k|k')$  is the probability that a neighbor of a node of degree  $k'$  has degree  $k$  and  $m_{kk'}$  is the average number of triangles a  $kk'$ -link is part of. The term proportional to  $m_{kk'}$  discounts for contacts of a given individual that were already infected by someone else, due to the presence of triangles. In Eq. (3), we neglect higher order loops such as squares. The reproduction matrix has been previously used to study percolation on networks [22].

We express the average number  $Z_n$  of infected individuals at generation  $n \geq 1$  in terms of  $M_{kk'}$  by summing over the degrees of individuals at each generation:

$$Z_n = \sum_{k_1 \dots k_n} M_{k_n k_{n-1}} M_{k_{n-1} k_{n-2}} \dots M_{k_2 k_1} k_1 P(k_1). \quad (4)$$

At the first generation, we obtain  $Z_1 = \bar{k}$ . For large  $n$ , we have  $Z_n \sim R^n$ , where we identify the reproduction number  $R$  as the leading eigenvalue of  $M_{kk'}$ . The associated right eigenvector  $v_{k'}$  represents the degree distribution of infected individuals [20].

In the simple case of an unclustered network ( $m_{kk'} = 0$  for all links) in which the degrees of connected nodes are

uncorrelated, we have

$$R = R_0 = \frac{\overline{k^2} - \bar{k}}{\bar{k}}, \quad (5)$$

where the bar represents an average over the degree distribution. Equation (5) is a classic result [7, 8, 23]. We seek to extend it to the general case of clustered and correlated networks. We quantify degree correlations between connected nodes by the assortativity coefficient  $r = 1/\sigma_r^2(\sum_{kk'} kk' P(k, k') - (\overline{k^2}/\bar{k})^2)$ , with  $\sigma_r^2 = \overline{k^3}/\bar{k} - (\overline{k^2}/\bar{k})^2$  [20]. We find that, for small clustering and assortativity coefficients, the effective reproduction number is expressed by

$$R_{\text{pert}} = (1 - r)(R_0 - m_1) + r \left( \frac{\frac{k(k-1)^2}{\bar{k}} - 2m_2 + m_1^2}{R_0 - m_1} \right), \quad (6)$$

where  $c_k$  is the probability that two neighbors of a node of degree  $k$  are themselves connected,  $m_1 = \overline{k(k-1)c_k}/\bar{k}$  is the average number of triangles a link is part of, and  $m_2 = \overline{k(k-1)^2 c_k}/\bar{k}$ . We obtained Eq. (6) by a perturbative expansion in  $r$  [20].

We compare  $R_{\text{pert}}$  given by Eq. (6) with the maximum eigenvalue  $R$  of the matrix  $M_{kk'}$  for different network models, see Table I. The relative difference between  $R$  and  $R_{\text{pert}}$  is within 2% for all the models we considered, except for Barabási-Albert with parameter  $m = 1$  (20.6%) and  $m = 2$  (7.1%), where  $m$  represents the number of nodes a new node attaches to. Approximating  $R$  with  $R_0$  as given by Eq. (5) leads to substantially larger errors, supporting that clustering and assortativity play an important role. Here and in the following, when computing  $R_{\text{pert}}$  using Eq. (6) and  $R_0$  using Eq. (5) for a given network, we always interpret the averages as empirical averages. With this choice, moments of the degree distribution remain finite even in very heterogeneous networks. In practical cases, Eq. (6) predicts that  $R_{\text{pert}}$  increases with the assortativity  $r$ . Accordingly, assortativity lowers the epidemic threshold, as previously known for the unclustered case [24]. However, this dependence is usually weak, unless the degree distribution has heavy tails. In contrast, clustering substantially reduces  $R_{\text{pert}}$ . For this reason, we find that  $R_0$  overestimates  $R$  in all the synthetic networks we considered.

*Network Euler-Lotka equation.* We now use our estimate of  $R$  to predict how epidemics spread in time. The average total number  $I_k(t)$  of infected individual of degree  $k$  at time  $t$  is governed by the renewal equation

$$\dot{I}_k(t) = \sum_{k'} \int_0^t \dot{I}_{k'}(t - \tau) M_{kk'} \psi(\tau) d\tau. \quad (7)$$

Equation (7) extends Eq. (1) to complex networks. Assuming exponential growth,  $\dot{I}_{k'}(u) \propto v_{k'} e^{\Lambda t}$ , we obtain

TABLE I. Reproduction numbers. Here,  $R$  is the numerically computed leading eigenvalue of Eq. (3). The expressions of  $R_0$  and  $R_{\text{pert}}$  are given by Eq. (5) and Eq. (6), respectively. To assess the impact of assortativity and clustering, we also compute  $R_{\text{pert}}$  for  $r = 0$  and for  $\bar{c} = \sum_k c_k P(k) = 0$ . BA $_m$ : Barabási-Albert with parameter  $m$ . ER $_d$ : Erdős-Rényi with mean degree  $d$ . WS $_{k,p}$ : Watts-Strogatz starting from a 1D lattice with  $k$  nearest neighbors and rewiring probability  $p$ .

Network	$R_0$	$R$	$R_{\text{pert}}$	$R_{\text{pert}}^{(r=0)}$	$R_{\text{pert}}^{(\bar{c}=0)}$	$r$	$\bar{c}$
BA $_1$	13.9	8.5	6.8	13.9	6.6	-0.011	0
BA $_2$	20.4	15.5	14.4	20.3	14.2	-0.008	0.0001
BA $_{12}$	85.4	80.8	79.5	83.6	80.4	-0.004	0.0003
ER $_6$	6.0	6.0	6.0	6.0	6.0	0.001	0.000
WS $_{8,2}$	7.2	4.9	4.9	4.9	7.0	-0.022	0.334
WS $_{6,2}$	5.2	3.6	3.6	3.6	5.0	-0.029	0.315

for large time

$$\frac{1}{R} = \langle e^{-\Lambda \tau} \rangle, \quad (8)$$

where  $\langle \dots \rangle$  denotes an average over  $\psi(\tau)$ . We call Eq. (8) the network Euler-Lotka equation.

We shall use Eq. (8) as an implicit relation for the unknown  $\Lambda$ , and call  $\Lambda_{\text{EL}}$  the solution of the equation. We can also explicitly express  $\Lambda$  from Eq. (8), but only in an approximate way. In particular, using the first two moments of  $\psi(\tau)$ , we obtain

$$\Lambda \approx \frac{\ln R}{\langle \tau \rangle} + (\ln R)^2 \frac{\sigma^2}{2\langle \tau \rangle^3}, \quad (9)$$

where  $\sigma^2 = \langle \tau^2 \rangle - \langle \tau \rangle^2$ , see [20]. An alternative is to combine Eq. (8) with the Jensen inequality, that states that  $\langle e^{-\Lambda \tau} \rangle \geq e^{-\Lambda \langle \tau \rangle}$ . This leads to the lower bound  $\Lambda \geq (\ln R)/\langle \tau \rangle$ . This bound is saturated when  $\psi(\tau)$  is a Dirac delta function.

*Synthetic networks.* The network Euler-Lotka equation successfully predicts the rate of epidemic spreading on synthetic complex networks, Fig. 2a and Fig. 2b. Our battery of tests includes a range of models characterized by different degree distribution, assortativity, and clustering. For each model, we use three different generation time distributions, see Fig. 2c. This choice qualitatively affect the epidemics. In particular, for peaked distributions, the exponential growth appears modulated by oscillations (Fig. 2a), since early generations of the epidemic are nearly synchronised. To extrapolate the leading exponential behavior from these curves, we fit them to a generalised logistic function

$$I(t) = \frac{N}{(1 + ((N/I_0)^\nu - 1) e^{-\Lambda_0 \nu t})^{1/\nu}}, \quad (10)$$

where  $N$  is the size of the network and  $I_0$ ,  $\Lambda_0$ , and  $\nu$  are free parameters, see [20]. Expanding Eq. (10) for small  $t$  we obtain  $\log I(t) \approx \log I_0 + t \Lambda_0 [1 - (I_0/N)^\nu]$ . This leads

us to define the finite-size growth rate  $\Lambda_{\text{FIT}} = \Lambda_0(1 - \eta)$  and the finite-size parameter  $\eta = (I_0/N)^\nu \in [0, 1]$ . The parameter  $\eta$  is also a measure of deviations from an exponential behavior, see [20].

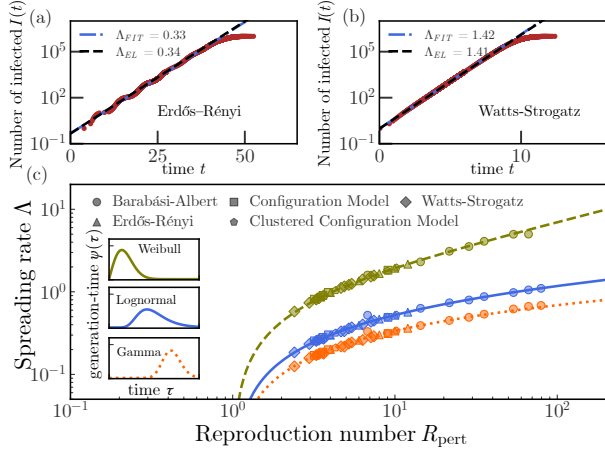


FIG. 2. Network Euler-Lotka equation predicts the epidemic spreading rate on synthetic networks. (a) and (b): Average trajectory  $I(t)$  over 500 realizations (red),  $\Lambda_{\text{FIT}}$  (blue dot-dashed) and  $\Lambda_{\text{EL}}$  (black dashed; based on  $R_{\text{pert}}$ , Eq. (6)) for Erdős-Rényi ( $N = 10^6$ ,  $\bar{k} = 4$ ) network with Gamma-distributed infection times and Watts-Strogatz network with Weibull-distributed infection times. (c) Solution of Eq. (8) compared with simulations for various networks of sizes up to  $10^6$ , see Ref. [20] for details.

When computing  $\Lambda_{\text{EL}}$ , we set  $R = R_{\text{pert}}$  as defined in Eq. (6) as the reproduction number. As expected, the predictions are considerably worse if we instead use  $R_0$ , see [20]. The difference between  $\Lambda_{\text{FIT}}$  and  $\Lambda_{\text{EL}}$  is within 6% for all networks, see Fig. 2c. The only exception is the Barabási-Albert model with parameter  $m = 1$  (average error 15%). One explanation for this discrepancy is that the exponential regime for this model is not well defined for  $N \rightarrow \infty$ , since  $\bar{k}^2$  diverges in this limit. Another explanation is that, for  $m = 1$ ,  $R_{\text{pert}}$  does not accurately match the leading eigenvalue of the reproduction matrix (see Table I).

*Real-world networks.* We apply the network Euler-Lotka equation to a large set of social, biological, technological, and transportation networks. These real-world networks often exhibit more complex structures than synthetic networks, with tightly linked communities, strong degree-correlation and broad tails in the degree distribution. Although they constitute a challenging test, the network Euler-Lotka equation holds well, see Fig. 3a and Fig. 3b for examples.

More generally, we find that  $\Lambda_{\text{EL}}$  well matches  $\Lambda_{\text{FIT}}$  whenever the finite-size parameter  $\eta$  detects a clear exponential regime, see Fig. 3c. Although some of these networks are highly clustered, using  $R_{\text{pert}}$  as expressed by Eq. (6) does not perform worse than  $R$  [20]. In Fig. 3c, we have omitted three road networks, for which the fit

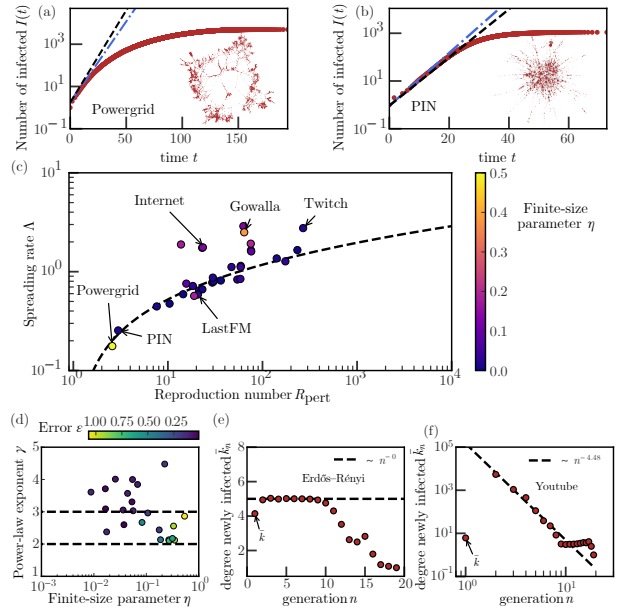


FIG. 3. Network Euler-Lotka equation predicts the epidemic spreading rate on real-world networks. We obtained  $I(t)$  by averaging 500 simulations using log-normal infection times for each network from Refs. [25–27] with at least 1000 nodes [20]. (a) and (b): Average trajectory  $I(t)$  (red),  $\Lambda_{\text{FIT}}$  (blue dot-dashed) and  $\Lambda_{\text{EL}}$  (black dashed) for powergrid and PIN networks. (c) Exponential spreading rate  $\Lambda_{\text{EL}}$  (dashed line) versus  $\Lambda_{\text{FIT}}$  (markers). (d) Degree distribution tail exponent ( $\gamma$ ) and finite-size parameter ( $\eta$ ) affect the estimation error  $\varepsilon = 2|\Lambda_{\text{FIT}} - \Lambda_{\text{EL}}|/(\Lambda_{\text{FIT}} + \Lambda_{\text{EL}})$ . Each dot represents a network, dashed lines mark the scale-free region  $2 < \gamma \leq 3$ . (e) and (f): Average degree  $\bar{k}_n$  of infected individuals at  $n$ -th generation for (a) Erdős-Rényi ( $N = 10^6$ ,  $\bar{k} = 4$ ) and (b) Youtube (scale-free,  $\gamma \approx 2.2$ ). Dashed lines represent power-law fits for  $n \in [1, 6]$ .

of Eq. (10) fails to converge. However, a function of the form  $\bar{I}(t) \sim t^\beta$  well fits the epidemic trajectories in these cases [20], likely because these networks are embedded in a two-dimensional physical space (see [28]).

For networks in which  $\eta < 0.5$ , the predictions of Eq. (8) using  $R_{\text{pert}}$  are more accurate than those using  $R_0$ . However, for larger values of  $\eta$ ,  $R_0$  performs slightly better on average [20]. Even in these cases,  $R_{\text{pert}}$  provides a better approximation of  $R$  [20]. The advantage of  $R_0$  for large  $\eta$  might be due to a compensatory effect: using  $R_0$  tends to overestimate  $R$ , while the network Euler-Lotka equation tends to underestimate  $\Lambda$  compared to  $\Lambda_{\text{FIT}}$ .

All of the networks where the prediction error is large are scale-free and characterized by a large value of  $\eta$ , see Fig. 3d. Here, scale-free means that the tail of the degree distribution scales as  $k^{-\gamma}$ , with  $\gamma \leq 3$ , see [29] and [20]. In contrast, the error is weakly affected by clustering [20]. The error for scale-free networks can be explained by the early infection of hubs, which depletes the tail of the degree distribution. In networks that are not scale-free,

we find that the average degree of infected individual is constant among generations as expected (Fig. 3e). In contrast, we find this average degree to decay as a power law in scale-free networks (Fig. 3f), leading to a non-steady spreading.

*Discussion.* In this Letter, we have related the exponential spreading rate of an epidemic on a complex network with the infectiousness and the network structure. Our theory accurately predicts the spreading rate on a wide range of synthetic and real-world networks, aside from scale-free networks where the exponential regime is hindered by finite-size effects.

When analyzing the early stage of real epidemics, departure from an exponential spreading is often interpreted as a consequence of behavioral response or containment measures (see, e.g., [30]). Our results show that non-exponential epidemic trajectories are common in heavy-tailed networks, thus providing an alternative explanation for these observations.

The classic Euler-Lotka equation is often used to estimate  $R$  in real epidemics. However, this approach is often inaccurate, because of difficulties in estimating both  $\Lambda$  and the infectiousness distribution (see, e.g., [31–33]). For this reason, approaches based on contact tracing have been developed [34, 35]. Our theory paves the way to use basic structural information on the interaction networks to directly estimate  $R$ .

We have focused for simplicity on static networks. Epidemic dynamics are more complex in temporal networks [36], for example due bursty social interactions [37]. Interactions could be also weighted, corresponding to contacts of different duration and intensity [38]. Our approach is flexible enough to be extended to these cases.

We thank C. Castellano and I. Neri for comments on a preliminary version of this manuscript. We thank Joshua Weitz for discussions. We are grateful for the help and support provided by the Scientific Computing and Data Analysis section of Core Facilities at OIST.

---

\* simone.pigolotti@oist.jp

- [1] C. Buckee, A. Noor, and L. Sattenspiel, *Nature* **595**, 205 (2021).
- [2] S. Patwardhan, V. K. Rao, S. Fortunato, and F. Radicchi, *Physical Review X* **13**, 041054 (2023).
- [3] C. Granell and P. J. Mucha, *Physical Review E* **97**, 052302 (2018).
- [4] S. Kumar, S. Jha, and S. K. Rai, *Indian Journal of Public Health* **64**, 139 (2020).
- [5] K. Sneppen, R. J. Taylor, and L. Simonsen, *MedRxiv*, 2020 (2020).
- [6] M. Newman, *Networks* (Oxford university press, 2018).
- [7] R. Pastor-Satorras and A. Vespignani, *Physical Review Letters* **86**, 3200 (2001).
- [8] M. E. Newman, *Physical Review E* **66**, 016128 (2002).
- [9] R. Pastor-Satorras, C. Castellano, P. Van Mieghem, and A. Vespignani, *Reviews of Modern Physics* **87**, 925 (2015).
- [10] M. Barthélemy, A. Barrat, R. Pastor-Satorras, and A. Vespignani, *Journal of theoretical biology* **235**, 275 (2005).
- [11] M. Pósfai and A.-L. Barabási, *Network Science* (Citeseer, 2016).
- [12] E. Ravasz and A.-L. Barabási, *Physical Review E* **67**, 026112 (2003).
- [13] N. C. Grassly and C. Fraser, *Nature Reviews Microbiology* **6**, 477 (2008).
- [14] J. S. Weitz, S. W. Park, C. Eksin, and J. Dushoff, *Proceedings of the National Academy of Sciences* **117**, 32764 (2020).
- [15] M. Barthélemy, A. Barrat, R. Pastor-Satorras, and A. Vespignani, *Physical Review Letters* **92**, 178701 (2004).
- [16] S. Moore and T. Rogers, *Physical Review Letters* **124**, 068301 (2020).
- [17] W. Merbis and I. Lodato, *Physical Review E* **105**, 044303 (2022).
- [18] C. Rose, A. J. Medford, C. F. Goldsmith, T. Vegge, J. S. Weitz, and A. A. Peterson, *Journal of Theoretical Biology* **528**, 110839 (2021).
- [19] H. Berestycki, B. Desjardins, J. S. Weitz, and J.-M. Oury, *Journal of Mathematical Biology* **86**, 60 (2023).
- [20] See Supplemental Material [url] for additional results and figures.
- [21] S. Hakki, J. Zhou, J. Jonnerby, A. Singanayagam, J. L. Barnett, K. J. Madon, A. Koycheva, C. Kelly, H. Houston, S. Nevin, *et al.*, *The Lancet Respiratory Medicine* **10**, 1061 (2022).
- [22] M. Á. Serrano and M. Boguná, *Physical Review E* **74**, 056115 (2006).
- [23] D. S. Callaway, M. E. Newman, S. H. Strogatz, and D. J. Watts, *Physical Review Letters* **85**, 5468 (2000).
- [24] A. V. Goltsev, S. N. Dorogovtsev, J. G. Oliveira, and J. F. Mendes, *Physical Review Letters* **109**, 128702 (2012).
- [25] A. Clauset, E. Tucker, and M. Sainz, “The Colorado Index of Complex Networks,” <https://icon.colorado.edu/> (2016).
- [26] J. Leskovec and A. Krevl, “SNAP Datasets: Stanford large network dataset collection,” <http://snap.stanford.edu/data> (2014).
- [27] J. Kunegis, in *Proc. Int. Conf. on World Wide Web Companion* (2013) pp. 1343–1350.
- [28] J. M. Moore, M. Small, G. Yan, H. Yang, C. Gu, and H. Wang, *Physical Review Letters* **132**, 237401 (2024).
- [29] I. Voitalov, P. Van Der Hoorn, R. Van Der Hofstad, and D. Krioukov, *Physical Review Research* **1**, 033034 (2019).
- [30] B. F. Maier and D. Brockmann, *Science* **368**, 742 (2020).
- [31] S. A. Lauer, K. H. Grantz, Q. Bi, F. K. Jones, Q. Zheng, H. R. Meredith, A. S. Azman, N. G. Reich, and J. Lessler, *Annals of Internal Medicine* **172**, 577 (2020).
- [32] L. Ferretti, C. Wymant, M. Kendall, L. Zhao, A. Nurtay, L. Abeler-Dörner, M. Parker, D. Bonsall, and C. Fraser, *Science* **368**, eabb6936 (2020).
- [33] H. Nishiura, N. M. Linton, and A. R. Akhmetzhanov, *International Journal of Infectious Diseases* **93**, 284 (2020).
- [34] S. Kojaku, L. Hébert-Dufresne, E. Mones, S. Lehmann, and Y.-Y. Ahn, *Nature Physics* **17**, 652 (2021).
- [35] P. Birello, M. Re Fiorentin, B. Wang, V. Colizza, and

- E. Valdano, *Nature Physics* , 1 (2024).
- [36] C.-R. Cai, Y.-Y. Nie, and P. Holme, *Physical Review Research* **6**, L022017 (2024).
- [37] A. V. Tkachenko, S. Maslov, T. Wang, A. Elbana, G. N. Wong, and N. Goldenfeld, *Elife* **10**, e68341 (2021).
- [38] L. Ferretti, C. Wymant, J. Petrie, D. Tsallis, M. Kendall, A. Ledda, F. Di Lauro, A. Fowler, A. Di Francia, J. Panovska-Griffiths, *et al.*, *Nature* **626**, 145 (2024).

# Supplementary information: Rate of epidemic spreading on complex networks

Samuel Cure, Florian G. Pflug, and Simone Pigolotti

*Biological Complexity Unit, Okinawa Institute of Science and Technology, Onna, Okinawa 904-0495, Japan.*

This document contains additional mathematical derivations and figures complementing the paper “Rate of epidemic spreading on complex networks” (from now on the “Main Text”). The document is organized as follows. Section I extends our theory to the case in which the probability  $p_\psi$  that an infected individual infects one of its neighbors is less than one. Section II presents a derivation of the expression for the reproduction number  $R_{\text{pert}}$  (Eq. 6 in the Main Text). Section III presents an alternative derivation of the Euler-Lotka equation (Eq. 8 in the Main Text) based on large deviation theory. We use this alternative derivation to find an approximate, but explicit expression for the exponential spreading rate (Eq. 9 in the Main Text). Section IV presents additional details on the fitting procedure of the generalized logistic equation, and additional results showing that the parameter  $\eta$  correctly describes deviations from an exponential regimes. Section V presents details on our numerical simulations, including additional details on the synthetic network models and real-world networks, expression of the generation time distributions  $\psi(\tau)$ , and details on the numerical algorithms. In this section we also present complementary results, such as the average epidemic trajectories for all the networks we considered in the Main Text. Finally, Section VI describes our method to fit the exponent  $\gamma$  characterizing the tails of the degree distribution.

## CONTENTS

I. Non-normalized generation-time distribution	2
A. Uncorrelated case	2
B. Correlated case	2
II. Explicit calculation of the reproduction number $R_{\text{pert}}$	3
III. Large deviation principle	6
A. Equation for the spreading rate	6
B. Gaussian approximation of the spreading rate	8
IV. Details on the fitting procedure and deviation from the exponential regime	8
V. Simulations of Epidemics on Networks	8
A. Generating synthetic networks	8
B. Real-world networks	9
C. Simulations	10
D. Power-law fit of the trajectories	11
E. Trajectories Synthetic Networks	13
1. Gamma	13
2. Lognormal	17
3. Weibull	21
F. Trajectories real networks	25
1. Lognormal	25
2. Gamma	28
3. Weibull	31
G. Comparison between estimates of the reproduction number	34
VI. Estimating the tail of the degree distribution	34
References	37

## I. NON-NORMALIZED GENERATION-TIME DISTRIBUTION

In the Main Text, we presented our theory in the case in which the integral  $p_\psi = \int_0^\tau \psi(\tau') d\tau'$ , representing the probability of spreading the infection via a given link, is equal to one. In this section, we extend the theory to the general case where  $0 < p_\psi \leq 1$ .

When  $p_\psi = 1$  the reproduction number  $R$  solely depends on the topology of the network. However, for  $0 < p_\psi < 1$ ,  $R$  also depends on  $p_\psi$ .

In our model, the infection spreads through every link at most once. The case in which the infection fails to spread via a specific link is equivalent to a case in which the link did not exist in the first place. This means that the case  $p_\psi < 1$  can be studied by removing links with uniform probability  $(1 - p_\psi)$ . This procedure alters the degree distribution of the network, which becomes

$$P^{\text{new}}(k) = \sum_q \binom{q}{k} p_\psi^k (1 - p_\psi)^{q-k} P(q). \quad (1)$$

### A. Uncorrelated case

When the network is unassortative and unclustered, the reproduction number scales linearly with  $p_\psi$ :

$$\sum_k (k^2 - k) P^{\text{new}}(k) = p_\psi^2 (\overline{k^2} - \bar{k}) \quad (2)$$

$$\sum_k k P^{\text{new}}(k) = p_\psi \bar{k} \quad (3)$$

$$\implies R_0^{\text{new}} = p_\psi R_0, \quad (4)$$

where  $R_0 = \overline{k^2}/\bar{k} - 1$ . Thus, the epidemic threshold ( $R_0 > 1$ ) is reached when:

$$p_\psi > \frac{\bar{k}}{k^2 - \bar{k}}. \quad (5)$$

This relation recovers the classic result of epidemic threshold on uncorrelated networks [1, 2].

However, this linear relation does not hold, in general, for clustered or assortative networks. Triangles are vulnerable to link removal since all three links need to remain for a triangle to be preserved. If a given link belongs on average to  $m_1$  triangles, after link removal it belongs on average to only  $m_1 p_\psi^2$  triangles. Therefore, we expect the new reproduction number (in the absence of degree correlations) to scale as:

$$R^{\text{new}(r=0)} = p_\psi R_0 - m_1 p_\psi^2. \quad (6)$$

We test Eq. (6) on a Watts–Strogatz network, which is clustered and has almost no correlation in the connected degrees ( $r \approx 0$ ), see Fig. 1. We observe that Eq. (6) captures well the behaviour of the spreading rate. In conclusion, the effect of link removal reduces the reproduction number while also weakening the effect of clustering. The impact on clustering is not strong enough to observe an increase in the reproduction number as  $p_\psi$  is decreased.

### B. Correlated case

Under node removal with uniform probability  $1 - p_\psi$ , the assortativity  $r$  changes as

$$r^{\text{new}} = r \left( 1 + \frac{p_\psi R_0}{1 - p_\psi \sigma_r^2} \right)^{-1}, \quad (7)$$

where  $\sigma_r^2 = \overline{k^3}/\bar{k} - (\overline{k^2}/\bar{k})^2$ . Equation (7) is derived in Ref. [3]. Similarly to the derivation in subsection IA, we obtain

$$\frac{\sum_k P^{\text{new}}(k) k(k-1)^2}{\sum_{k'} k' P^{\text{new}}(k')} = p_\psi^2 \frac{\overline{k(k-1)^2}}{\bar{k}} + R_0 p_\psi (1 - p_\psi) \quad (8)$$

and

$$m_2^{\text{new}} \rightarrow p_\psi^3 m_2 + p_\psi^2 (1 - p_\psi) m_1. \quad (9)$$

Therefore, we have

$$R_{\text{pert}}^{\text{new}} = p_\psi (R_0 - m_1 p_\psi) (1 - r^{\text{new}}) + r^{\text{new}} (1 - p_\psi) + \quad (10)$$

$$\frac{r^{\text{new}}}{R_0 - m_1 p_\psi} \left( p_\psi \frac{\overline{k(k-1)^2}}{\overline{k}} - 2p_\psi^2 m_2 - p_\psi m_1 (1 - p_\psi + m_1 p_\psi^2) \right) + \mathcal{O}(r^2), \quad (11)$$

where  $r^{\text{new}}$  is given by Eq. (7). To test Eq. (10), we simulate repeated epidemics with a Gamma generation-time distribution while varying  $p_\psi$  on two different network. First, we consider a synthetic network that is disassortative and exhibit a heavy-tail in its degree distribution, see Fig. 2a. Second, we consider the Amazon network (see Sec. V B), which presents assortativity, a heavy tail, and clustering. We find that our theory is in good agreements with the simulations, until  $p_\psi$  becomes too small. For small  $p_\psi \approx 0.2$ , the network is too close to the percolation threshold and the generalized logistic fit becomes less reliable.

## II. EXPLICIT CALCULATION OF THE REPRODUCTION NUMBER $R_{\text{pert}}$

In this section, we derive the expression of the reproduction number  $R_{\text{pert}}$ . Our strategy is to approximate the eigenvalue by assuming weak clustering and treating the degree correlations as a perturbation of the uncorrelated case.

We recall that degree correlations are summarised by the assortativity  $r$  [4], defined as the Pearson correlation coefficient of the degrees of connected nodes:

$$r = \frac{1}{\sigma_r^2} \sum_{kk'} \left[ kk' P(k, k') - \frac{k^2 k'^2}{\overline{k}^2} P(k) P(k') \right], \quad (12)$$

where  $\sigma_r^2 = \overline{k^3}/\overline{k} - (\overline{k^2}/\overline{k})^2$  ensures that  $-1 \leq r \leq 1$  and  $P(k, k') = k' P(k|k') P(k') / \overline{k}$  is the probability that a randomly chosen edge connects nodes of degrees  $k$  and  $k'$ .

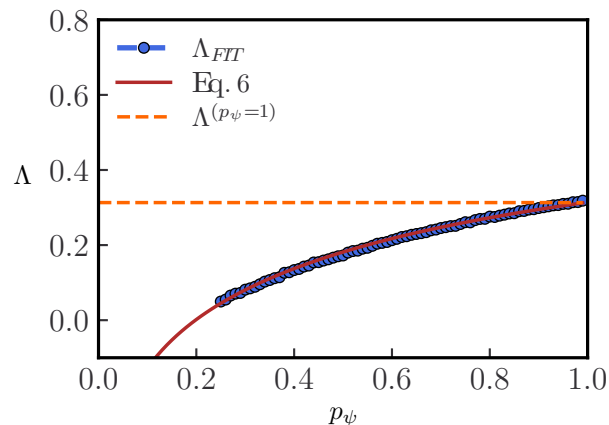


FIG. 1: **Effect of non-normalised generation-time on the spreading rate.** We generate a Watts–Strogatz network with parameter  $k = 6$  and rewiring probability  $p = 0.3$ . We then simulate the average epidemic trajectory over 100 trajectories using a Gamma generation-time distribution (Eq. (64)) but the transmission via a given link only occurs with probability  $p_\psi$ . We repeat this for all  $p_\psi$  and measure the empirical spreading rate (blue markers). We compare it with the spreading rate obtained using Eq. (6) (red line) and include the spreading rate in the case where  $p_\psi = 1$  (orange dashed line).

We now analyse the clustering measure  $m_{kk'}$ . While being a measure of clustering,  $m_{kk'}$  also contains information on the degree correlation of connected nodes. In contrast, the degree dependent clustering coefficient  $c_k$  is independent of degree correlations [5]. This coefficient is related to  $m_{kk'}$  as  $(k-1)c_k = \sum_{k'} m_{kk'} P(k'|k)$ . If we assume that  $m_{kk'}$  factorises into  $k$  and  $k'$ -dependent factors, we can express  $m_{kk'}$  as

$$m_{kk'} = \frac{(k-1)c_k(k'-1)c_{k'}}{m_1} \quad (13)$$

where  $m_1 = \overline{k(k-1)c_k/\bar{k}}$ . In particular, this factorisation is justified in the weak clustering limit [5]. Using this expression, we rewrite the reproduction matrix as

$$M_{kk'} = (k'-1) \left[ 1 - c(k') \frac{(k-1)c_k}{m_1} \right] P(k|k') \quad (14)$$

To further simplify the problem, we neglect the dependence on  $k$  of the probability that a node of degree  $k'$  connected to a node of degree  $k$  is part of a triangle. This amounts to assuming  $(k-1)c_k/m_1 = 1$ , so that Eq. (14) becomes

$$M_{kk'} = (k'-1)[1 - c(k')]P(k|k'). \quad (15)$$

We now treat  $r$  as a small perturbation parameter and express the leading eigenvalue using perturbation theory. In the unperturbed case  $r = 0$ , the reproduction matrix  $M_{kk'}$  has a single non-zero eigenvalue  $R_{\text{unper}}$  with left and right eigenvectors  $u_k^{(0)}$  and  $v_k^{(0)}$ , normalized such that  $\sum_k v_k^{(0)} u_k^{(0)} = 1$ :

$$R_{\text{unper}} = \frac{\overline{k^2} - \bar{k}}{\bar{k}} - m_1, \quad (16)$$

$$u_k^{(0)} = \frac{(k-1)(1-c_k)}{R_{\text{unper}}} \quad (17)$$

$$v_k^{(0)} = \frac{k}{\bar{k}} P(k). \quad (18)$$

At the order of  $\mathcal{O}(r)$ , the leading eigenvalue is given by:

$$R_{\text{pert}} = R_{\text{unper}} + r \sum_{kk'} u_k^{(0)} \delta M_{kk'} v_{k'}^{(0)} + \mathcal{O}(r^2), \quad (19)$$

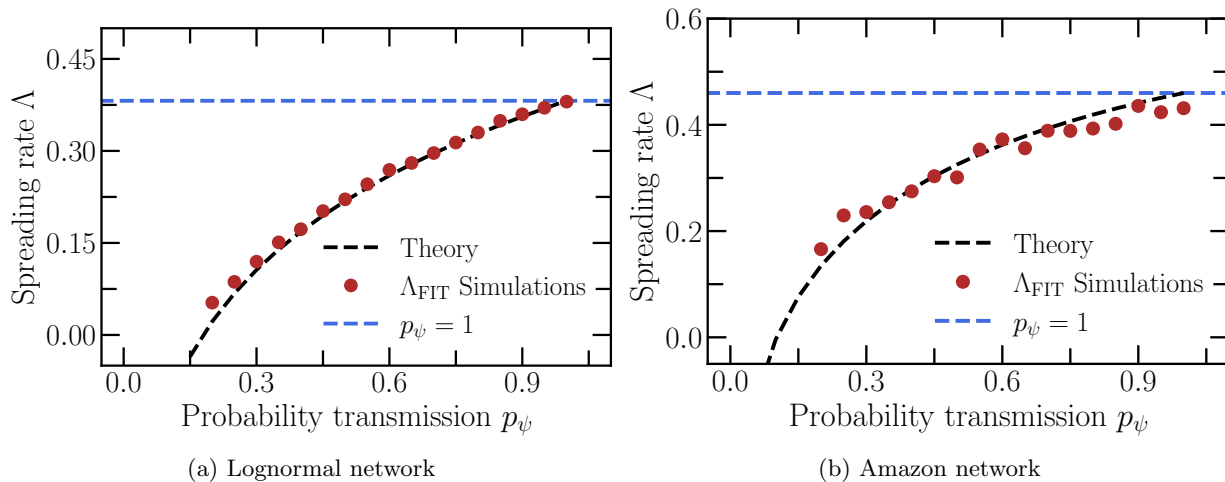


FIG. 2: **Impact of the transmission probability on the epidemic spreading rate.** For each  $p_\psi$  (red markers), we simulate the average epidemic trajectory over 100 trajectories with infection times that are Gamma distributed (Eq. (64)). We run the simulations on a network whose degree are lognormally distributed (Eq. (65)), Panel (a). We repeat this for the Amazon network, Panel (b). The black dashed line represent the solution of the Euler-Lotka equation when we use  $R_{\text{pert}}$  from Eq. (10).

where

$$\sum_{kk'} u_k^{(0)} \delta M_{kk'} v_{k'}^{(0)} = \frac{1}{R_{\text{unper}}} \sum_{kk'} \left[ (k-1)(1-c_k)(k'-1)(1-c(k')) P^{(1)}(k|k') P(k') \frac{k'}{\bar{k}} \right] - R_{\text{unper}}. \quad (20)$$

Expanding the terms involving clustering coefficients, we separate the sum in four distinct terms. The first three are

$$\sum_{kk'} (k-1)(k'-1) P^{(1)}(k|k') P(k') \frac{k'}{\bar{k}} = \frac{\overline{k(k-1)^2}}{\bar{k}}. \quad (21)$$

$$\sum_{kk'} c_k (k-1)(k'-1) P^{(1)}(k|k') P(k') \frac{k'}{\bar{k}} = \frac{\overline{k(k-1)^2 c_k}}{\bar{k}}. \quad (22)$$

$$\sum_{kk'} c_{k'} (k-1)(k'-1) P^{(1)}(k|k') P(k') \frac{k'}{\bar{k}} = \frac{\overline{k(k-1)^2 c_k}}{\bar{k}}. \quad (23)$$

Eq. (22) and Eq. (23) yield the same result due to degree detailed balance, which holds because links are undirected. Indeed, we have

$$P(k|k') P(k') \frac{k'}{\bar{k}} = P(k'|k) P(k) \frac{k}{\bar{k}} \quad (24)$$

$$\left( \frac{k}{\bar{k}} P(k)(1-r) + r(P^{(1)}(k|k')) \right) P(k') \frac{k'}{\bar{k}} = \left( \frac{k'}{\bar{k}} P(k')(1-r) + r(P^{(1)}(k'|k)) \right) P(k) \frac{k}{\bar{k}} \quad (25)$$

$$P(k') \frac{k'}{\bar{k}} \frac{k}{\bar{k}} P(k)(1-r) + r(P^{(1)}(k|k') P(k') \frac{k'}{\bar{k}}) = P(k) \frac{k}{\bar{k}} \frac{k'}{\bar{k}} P(k')(1-r) + r(P^{(1)}(k'|k) P(k) \frac{k}{\bar{k}}) \quad (26)$$

$$P^{(1)}(k|k') P(k') \frac{k'}{\bar{k}} = P^{(1)}(k'|k) P(k) \frac{k}{\bar{k}}. \quad (27)$$

The fourth term in the sum reads

$$\sum_{kk'} c_k c_{k'} (k-1)(k'-1) P^{(1)}(k|k') P(k') \frac{k'}{\bar{k}}. \quad (28)$$

To evaluate this sum, we first make use of the fact that:

$$c_k (k-1) = \sum_{k'} m_{kk'} P(k'|k). \quad (29)$$

This relation holds for any network [6]. Since Eq. (29) is valid for any network, it also holds when  $m_{kk'}$  factorises, i.e., when  $m_{kk'} = c_k (k-1) c_{k'} (k'-1) / m_1$ . We then write Eq. (29) as

$$(k-1) c_k = \frac{1}{m_1} \sum_{k'} c_k (k-1) c_{k'} (k'-1) P(k'|k) \quad (30)$$

$$m_1 = \sum_{k'} c_{k'} (k'-1) P(k'|k) \quad (31)$$

$$m_1 = (1-r) \sum_{k'} c_{k'} (k'-1) \frac{k'}{\bar{k}} P(k') + r \sum_{k'} c_{k'} (k'-1) P^{(1)}(k'|k) \quad (32)$$

$$m_1 = (1-r) m_1 + r \sum_{k'} c_{k'} (k'-1) P^{(1)}(k'|k) \quad (33)$$

$$\implies \sum_{k'} c_{k'} (k'-1) P^{(1)}(k'|k) = m_1. \quad (34)$$

Thus, we express the last term as

$$\sum_{kk'} c_k (k-1) c_{k'} (k'-1) P^{(1)}(k|k') P(k') \frac{k'}{\bar{k}} = m_1^2. \quad (35)$$

Therefore, we write the leading eigenvalue as

$$R_{\text{pert}} = R_{\text{unper}}(1 - r) + \frac{r}{R_{\text{unper}}} \left( \frac{\overline{k(k-1)^2}}{\bar{k}} - 2m_2 + m_1^2 \right) + \mathcal{O}(r^2), \quad (36)$$

where we identify  $m_2 = \overline{k(k-1)^2 c_k / \bar{k}}$ .

We remark that  $m_2$  is indirectly related to the average degree of nodes being part of a triangle. After picking randomly a triangle in the network, we pick one of the three nodes. The probability that it has degree  $k$  is given by  $c_k(k-1)kP(k)/(m_1\bar{k})$ . Thus the average degree of a node belonging to a triangle is expressed by

$$\sum_k \frac{c_k(k-1)}{m_1} \frac{k^2}{\bar{k}} P(k) = \sum_k \frac{c_k(k-1)^2}{m_1} \frac{k}{\bar{k}} P(k) + \sum_k \frac{c_k(k-1)}{m_1} \frac{k}{\bar{k}} P(k) \quad (37)$$

$$= \frac{m_2}{m_1} + 1. \quad (38)$$

Finally, the first order correction of the right eigenvector associated to the unique leading eigenvalue is given by

$$v_k^{(1)} = v_k^{(0)} + \frac{r}{R_{\text{unper}}} \sum_{k'} \delta M_{kk'} v_{k'}^{(0)} + \mathcal{O}(r^2). \quad (39)$$

$$\sum_{k'} \delta M_{kk'} v_{k'}^{(0)} = \sum_{k'} (k' - 1)(1 - c_{k'}) P^{(1)}(k|k') \frac{k'}{\bar{k}} P(k') - \sum_{k'} (k' - 1)(1 - c_{k'}) P(k') P(k) \frac{kk'}{\bar{k}^2} \quad (40)$$

$$= \sum_{k'} (k' - 1)(1 - c_{k'}) P^{(1)}(k'|k) \frac{k}{\bar{k}} P(k) - R_{\text{unper}} \frac{k}{\bar{k}} P(k) \quad (41)$$

$$= (k - 1) \frac{k}{\bar{k}} P(k) - m_1 \frac{k}{\bar{k}} P(k) - R_{\text{unper}} \frac{k}{\bar{k}} P(k). \quad (42)$$

Therefore, we obtain

$$v_k^{(1)} = (1 - r) \frac{k}{\bar{k}} P(k) + \frac{r}{R_{\text{unper}}} ((k - 1) - m_1) \frac{k}{\bar{k}} P(k) + \mathcal{O}(r^2). \quad (43)$$

### III. LARGE DEVIATION PRINCIPLE

#### A. Equation for the spreading rate

The network Euler-Lotka equation is derived in the Main Text from the renewal equation. Here, we present an alternative derivation which relates the exponential spreading rate  $\Lambda$  to a large deviation principle. This derivation is slightly more lengthy but will permit us to derive an approximate explicit expression for  $\Lambda$ .

In a network of infinite size, we define the exponential spreading rate as

$$\Lambda = \lim_{t \rightarrow \infty} \frac{1}{t} \ln I(t), \quad (44)$$

provided that this limit exists. We first express the number of infected  $I(t)$  in terms of lineages. The epidemic starts with a single infected individual, which we call the root node, and the epidemic progresses as infected individuals spread the infection to their neighbours. We call a leaf a node that is infected but has not yet transmitted the disease to any of its neighbours. We define  $L(n, t)$  as the number of leaves at time  $t$  that are at a distance  $n$  from the root. The epidemic passed through  $n$  different nodes before reaching those leaves. The total number of leaves is always smaller or equal to the total number of infected, but grows exponentially at the same rate, so that

$$\Lambda = \lim_{t \rightarrow \infty} \frac{1}{t} \ln \sum_n L(n, t). \quad (45)$$

We express the total number of leaves in the limit  $t \rightarrow \infty$  as

$$\sum_n L(n, t) \approx \sum_n Z_n p_t(n), \quad (46)$$

where  $Z_n$  is the average number of nodes at a distance  $n$  from the root and  $p_t(n)$  is the probability that on a given lineage the infection has spread to a distance  $n$  by time  $t$ . This approximation holds on the assumption that lineages are independent, which is effectively the case for large time. Therefore, we obtain

$$\Lambda = \lim_{t \rightarrow \infty} \frac{1}{t} \ln \sum_n Z_n p_t(n). \quad (47)$$

This representation allows to separate the properties of the infection times and of the network:  $Z_n$  only depends on the structure of the network while  $p_t(n)$  only depends on  $\psi(\tau)$ . In the case where  $p_\psi = 1$  (see Sec. I), then  $Z_n$  can be interpreted as the number of newly infected at generation  $n$  and scales as  $Z_n \sim R^n$ , where  $R$  is the reproduction number. Therefore, we have

$$\Lambda = \lim_{t \rightarrow \infty} \frac{1}{t} \ln \langle R^n \rangle_n. \quad (48)$$

where  $\langle \dots \rangle_n$  represents the average over the distribution  $p_t(n)$ . In this representation, the variable  $n$  depends on  $t$  and can be interpreted as a counting process  $n(t)$  with generation-time  $\psi(\tau)$ , such that  $p_t(n)$  is the probability that a lineage is of size  $n$  at time  $t$ .

We now follow the same steps as in Ref. [7]. We define the variable  $\omega = n/t$ , so that  $\omega$  tends to a constant as  $t$  grows large. We say that  $\omega$  satisfies a large deviation principle if

$$p(\omega) \asymp e^{-tI^{(\omega)}(\omega)}, \quad (49)$$

where  $I^{(\omega)}(\omega)$  is called the rate function and where the sign  $\asymp$  means that as  $t \rightarrow \infty$  the dominant part of  $p(\omega)$  is the decaying exponential  $e^{-tI^{(\omega)}(\omega)}$ . Assuming that  $\omega$  satisfies a large deviation principle and that the rate function is convex, we apply the Gärtner-Ellis theorem

$$\Psi^{(\omega)}(q) = \sup_{\omega} [q\omega - I^{(\omega)}(\omega)], \quad (50)$$

where  $\Psi^{(\omega)}(q) = \lim_{t \rightarrow \infty} t^{-1} \ln \langle e^{qt\omega} \rangle_\omega$  is the the scaled cumulant generating function of  $\omega$ . Using in succession Eq. (48) and Eq. (50) we obtain

$$\Lambda = \sup_{\omega} [\omega \ln R - I^{(\omega)}(\omega)]. \quad (51)$$

To determine  $I^{(\omega)}(\omega)$  we remember that  $n(t)$  is described by a renewal process with generation-time  $\psi(\tau)$ . This means that its inverse  $t(n)$  is the sum of  $n$  I.I.D random variables distributed according to  $\psi(\tau)$ . Following Ref. [8], their rate functions are related by

$$I^{(\omega)}(x) = xI^{(t)}(1/x). \quad (52)$$

The scaled cumulant generating function of  $t$  can be expressed in terms of the probability density distribution of the infection times:

$$\Psi^{(t)}(q) = \lim_{n \rightarrow \infty} \frac{1}{n} \ln \langle e^{q \sum_{i=1}^n \tau_i} \rangle_\tau = \lim_{n \rightarrow \infty} \frac{1}{n} \ln \prod_{i=1}^n \langle e^{q\tau_i} \rangle_\tau = \ln \langle e^{q\tau} \rangle_\tau. \quad (53)$$

Applying once again the Gärtner-Ellis theorem, we find

$$I^{(t)}(1/x) = \sup_q \left[ \frac{q}{x} - \ln \langle e^{q\tau} \rangle_\tau \right]. \quad (54)$$

Combining this result with Eq. (52), we obtain

$$I^{(\omega)}(x) = x \sup_q \left[ \frac{q}{x} - \ln \langle e^{q\tau} \rangle_\tau \right]. \quad (55)$$

Substituting this in Eq. (51), we find

$$\Lambda = \sup_{\omega} \inf_q [\omega \ln R - q + \omega \ln \langle e^{q\tau} \rangle_\tau] \quad (56)$$

The extremality condition with respect to  $\omega$  is expressed by

$$\langle e^{q\tau} \rangle_\tau = \frac{1}{R} \quad (57)$$

Substituting it back in Eq. (56), we obtain  $\Lambda = -q^{\text{inf}}$ . Inserting this in the extremality condition gives the Euler-Lotka equation, Eq. (8) in the Main Text.

## B. Gaussian approximation of the spreading rate

In this section, we derive the approximate expression for  $\Lambda$ , Eq. (9) in the Main Text. In the limit  $t \rightarrow \infty$ , the distribution of the counting process  $n(t)$  tends to a Gaussian with mean  $\mu_n = t/\bar{\tau}$  and variance  $\sigma_n^2 = t\sigma^2/\bar{\tau}^3$  where  $\sigma^2 = \bar{\tau}^2 - \bar{\tau}^2$  is the variance of the generation-time distribution  $\psi(\tau)$ . Using Eq. (48), we thus represent  $\Lambda$  as an average over a Gaussian distribution:

$$\Lambda = \lim_{t \rightarrow \infty} \frac{1}{t} \ln \langle e^{n \ln R} \rangle_n \quad (58)$$

$$\approx \lim_{t \rightarrow \infty} \frac{1}{t} \ln \int_{-\infty}^{+\infty} e^{-\frac{(n-\mu_n)^2}{2\sigma_n^2} + n \ln R} dn \quad (59)$$

$$= \lim_{t \rightarrow \infty} \frac{1}{t} \ln \left( e^{\mu_n \ln R + ((\ln R)^2 \sigma_n^2)/2} \right) \quad (60)$$

$$= \frac{\ln R}{\langle \tau \rangle} + (\ln R)^2 \frac{\sigma^2}{2 \langle \tau \rangle^3}. \quad (61)$$

This formula illustrates how a larger variance contributes to a faster spreading epidemic, while a larger mean tends to slow down the spreading rate.

## IV. DETAILS ON THE FITTING PROCEDURE AND DEVIATION FROM THE EXPONENTIAL REGIME

When fitting epidemic trajectories using the generalized logistic equation (Eq. (10) in the Main Text), we fit the logarithm of  $I(t)$  versus  $t$ . In the fit we discard the initial times at which  $I(t) < \bar{k}$ . The reason is that the first  $\bar{k}$  infections should belong to the first generation  $Z_1$ , in which the average number of secondary infections per individual is  $\bar{k}$  rather than  $R$ .

If the epidemic spreading were purely exponential, then  $\ell(t) = \ln I(t)$  should appear as a perfectly linear function of  $t$ . To quantify the deviation from the exponential regime, we therefore consider the curvature  $\kappa$  of  $\ell(t)$ :

$$\kappa = \frac{\ell''(t)}{\left(1 + (\ell'(t))^2\right)^{3/2}}. \quad (62)$$

A large curvature indicates a marked deviation from exponential growth. To compare epidemic trajectories between networks, we compute the curvature as given by the generalized logistic equation for  $t = 0$ :

$$\kappa = \frac{\Lambda^2 \nu N^\nu (N^\nu - 1)}{(\Lambda^2 + (\Lambda^2 + 1) N^{2\nu} - 2\Lambda^2 N \eta^\nu)^{3/2}} + \mathcal{O}(t), \quad (63)$$

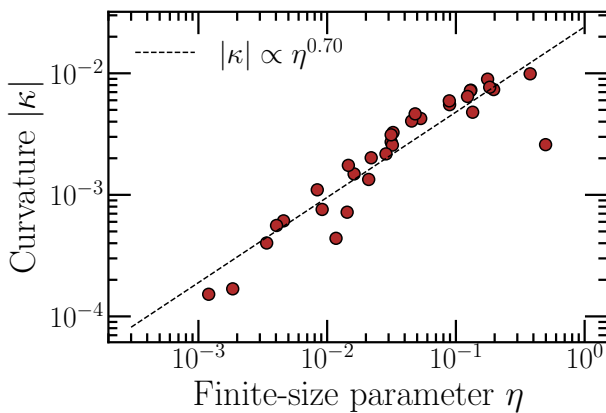
where we have set  $I_0 = 1$  to lighten the formula. We plot Eq. (63) as a function of  $\eta$  for various networks, see Fig. 3. We observe a strong log-log positive correlation between the curvature  $\kappa$  and the finite-size parameter  $\eta$ , supporting that the finite-size parameter can be taken as a proxy for the deviation from an exponential behaviour.

As explain in the main text, the network Euler-Lotka equation predicts the spreading rate  $\Lambda \text{EL}$  well except in some cases where the finite-size parameter  $\eta$  is large and the degree-distribution is scale-free. Clustering, on the other hand, does not affect the accuracy of the predicted spreading rate (Fig. (4)b).

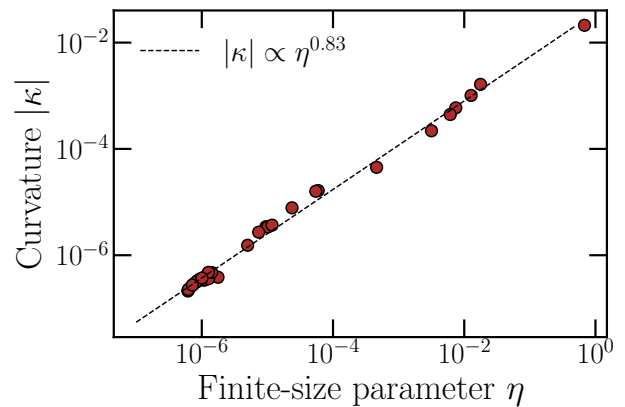
## V. SIMULATIONS OF EPIDEMICS ON NETWORKS

### A. Generating synthetic networks

We generate Erdős-Rényi, Barabási-Albert, and Watts-Strogatz networks using standard algorithms [9]. We also generate networks with arbitrary degree distribution by means of the configuration model [9] which consists in assigning to every node a number of stubs (half-links) according to a given degree sequence. Then each pair of stub is randomly chosen and connected via a link. Self-links and multiple links can appear, but their number is of the order  $\mathcal{O}(\infty/N)$ , where  $N$  is the number of nodes in the network. In the limit of large  $N$ , the network possesses a tree-like structure (no short loops) and the degrees of connected nodes are uncorrelated ( $r \approx 0$ ).



(a) Real-world Networks, Lognormal generation-time distribution.



(b) Synthetic Networks, Weibull generation-time distribution

FIG. 3: **Relationship between curvature and finite-size parameter.** For each epidemic trajectory, (a) real-world networks, (b) synthetic networks, we determine the parameters that best fit the generalised logistic function and compute  $\eta$  and  $\kappa$ . The Pearson correlation coefficient between  $\ln(\kappa)$  and  $\ln(\eta)$  is 0.92 in (a) and 0.99 in (b).

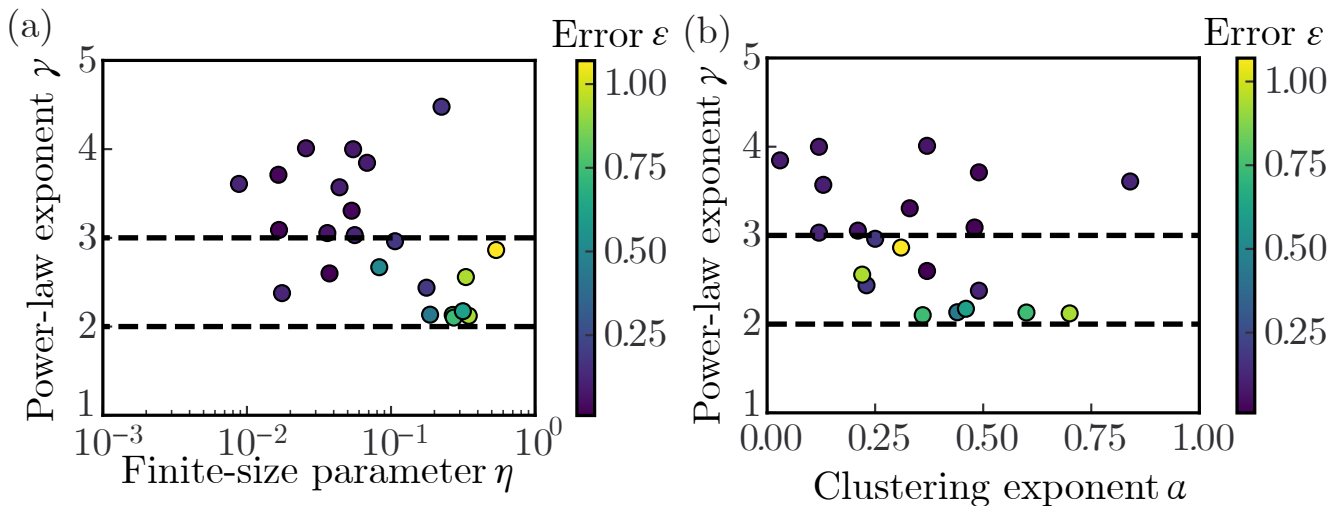


FIG. 4: Effect of degree distribution tail exponent ( $\gamma$ ), finite-size parameter ( $\eta$ ) and clustering coefficient ( $\alpha$ ) on the estimation error  $\varepsilon = 2|\Lambda_{\text{FIT}} - \Lambda_{\text{EL}}|/(\Lambda_{\text{FIT}} + \Lambda_{\text{EL}})$ . Each dot represents a network, dashed lines mark the scale-free region  $2 < \gamma \leq 3$ . (a) Effect of  $\gamma$  and  $\eta$  on  $\varepsilon$  (identical to Fig. 3d in the Main Text). (b) Effect of  $\gamma$  and  $\alpha$  on  $\varepsilon$ .

We tune the assortativity in a given network as follows. We choose two pairs of connected nodes  $a, b, c, d$ , arranged such that  $k_a \leq k_b \leq k_c \leq k_d$ . We rewire the links by forming new pairs  $a - b$  and  $c - d$  to increase assortativity, or  $a - d$  and  $b - d$  to decrease assortativity. This operation preserves the degree distribution while inducing degree correlation.

To generate networks with a tunable clustering coefficient, we implement an algorithm that generalises the configuration model [6]. In our implementation, we start with a degree sequence generated from a distribution  $P(k)$  and choose an exponent  $\alpha$  so that the number of triangles being part of a node of degree  $k$  is on average  $(k - 1)c_k$ , so that  $c_k = a(k - 1)^{-\alpha}$ . See Ref. [6] for more details.

## B. Real-world networks

We collected real networks available from various databases: SNAP [10], ICON [11] and KONECT [12]. We selected networks of size  $N > 1000$ , only possessing undirected links, not temporal, and not bipartite. The properties of the

TABLE I: Comparison of the properties of all considered synthetic networks.

Network	$N$	$r$	$\bar{c}$	$m_1$	$\bar{k}$	$R_0$	$R$	$R_{\text{pert}}$	Error
BA <sub>1</sub>	$1.0 \times 10^6$	-0.010	0.0	0.0	2.0	13.9	8.5	6.8	0.21
BA <sub>2</sub>	$1.0 \times 10^6$	-0.008	$1.2 \times 10^{-4}$	0.1	4.0	20.4	15.5	14.4	0.07
BA <sub>3</sub>	$1.0 \times 10^6$	-0.008	$1.3 \times 10^{-4}$	0.2	6.0	27.8	22.6	21.6	0.04
BA <sub>4</sub>	$1.0 \times 10^6$	-0.007	$1.4 \times 10^{-4}$	0.3	8.0	34.5	29.4	28.6	0.03
BA <sub>5</sub>	$1.0 \times 10^6$	-0.006	$1.8 \times 10^{-4}$	0.0	10.0	41.0	35.9	35.5	0.01
BA <sub>8</sub>	$1.0 \times 10^6$	-0.005	$2.2 \times 10^{-4}$	0.7	16.0	58.6	54.5	53.7	0.01
BA <sub>10</sub>	$1.0 \times 10^6$	-0.004	$2.6 \times 10^{-4}$	1.3	20.0	72.1	67.7	66.5	0.02
BA <sub>12</sub>	$1.0 \times 10^6$	0.004	$3.0 \times 10^{-4}$	1.8	24.0	85.4	80.8	79.5	0.02
ER <sub>4</sub>	$1.0 \times 10^6$	0.0	0.0	0.0	4.0	4.0	4.0	4.0	0.0
ER <sub>6</sub>	$1.0 \times 10^6$	0.0	0.0	0.0	6.0	6.0	6.0	6.0	0.0
ER <sub>8</sub>	$1.0 \times 10^6$	0.0	0.0	0.0	8.0	8.0	8.0	8.0	0.0
ER <sub>10</sub>	$1.0 \times 10^6$	-0.0	0.0	0.0	10.0	10.0	10.0	10.0	0.0
ER <sub>12</sub>	$1.0 \times 10^6$	0.0	0.0	0.0	12.0	12.0	12.0	12.0	0.0
ER <sub>10</sub> $\alpha = 0.2$	$1 \times 10^5$	0.06	0.1	1.0	10.0	10.0	9.0	9.1	0.01
ER <sub>4</sub> $\alpha = 2$	$1 \times 10^5$	0.04	0.1	0.2	4.1	4.0	4.0	3.9	0.02
ER <sub>4</sub> $\alpha = 0.5$	$1 \times 10^5$	0.04	0.2	0.6	4.1	4.0	3.4	3.5	0.02
LN <sub>4,1</sub> $\alpha = 0.5$	$1.0 \times 10^5$	0.01	0.2	0.6	4.5	3.7	3.2	3.2	0.01
LN <sub>4,1</sub> $\alpha = 2$	$1.0 \times 10^5$	0.02	0.1	0.1	4.5	3.7	3.6	3.6	0.0
LN <sub>10,12</sub>	$1.0 \times 10^6$	-0.0	0.0	0.0	10.0	10.2	10.2	10.2	0.0
LN <sub>4,1</sub>	$1.0 \times 10^6$	-0.0	0.0	0.0	4.0	3.3	3.3	3.3	0.0
BT <sub>2,4</sub>	$1.0 \times 10^5$	0.0	0.0	0.0	5.0	4.3	4.3	4.3	0.0
BT <sub>5,4</sub>	$1.0 \times 10^5$	-0.0	0.0	0.0	8.0	9.0	9.0	9.0	0.01
WS <sub>4,2</sub>	$1.0 \times 10^6$	-0.04	0.3	0.8	4.0	3.2	2.4	2.4	0.0
WS <sub>4,6</sub>	$1.0 \times 10^6$	-0.1	0.0	0.1	4.0	3.4	3.3	3.3	0.0
WS <sub>4,8</sub>	$1.0 \times 10^6$	-0.11	0.0	0.0	4.0	3.5	3.4	3.4	0.0
WS <sub>6,2</sub>	$1.0 \times 10^6$	-0.03	0.3	1.5	6.0	5.2	3.6	3.6	0.0
WS <sub>6,4</sub>	$1.0 \times 10^6$	-0.05	0.1	0.7	6.0	5.3	4.6	4.6	0.0
WS <sub>6,6</sub>	$1.0 \times 10^6$	-0.07	0.0	0.2	6.0	5.4	5.2	5.2	0.0
WS <sub>6,8</sub>	$1.0 \times 10^6$	-0.07	0.0	0.0	6.0	5.5	5.4	5.4	0.0
WS <sub>8,2</sub>	$1.0 \times 10^6$	-0.02	0.3	2.3	8.0	7.2	4.9	4.9	0.0
WS <sub>8,4</sub>	$1.0 \times 10^6$	-0.04	0.1	1.0	8.0	7.3	6.3	6.3	0.0
WS <sub>8,6</sub>	$1.0 \times 10^6$	-0.05	0.0	0.3	8.0	7.4	7.1	7.1	0.0
WS <sub>8,8</sub>	$1.0 \times 10^6$	-0.06	0.0	0.0	8.0	7.5	7.4	7.4	0.0

selected networks and their estimated reproduction number are listed in Table II.

### C. Simulations

We simulate the average trajectory of an epidemic over 500 trajectories for every network. We repeat the simulations for three different infection time distributions: a Gamma distribution with mean 7 and variance 1:

$$\psi_{\text{gam}}(\tau) = \frac{e^{-\frac{m\tau}{v}} \left(\frac{v}{m\tau}\right)^{-\frac{m^2}{v}}}{\tau \Gamma\left(\frac{m^2}{v}\right)}, \quad m = 7, v = 1; \quad (64)$$

a Log-normal distribution with mean 5 and variance 3:

$$\psi_{\text{log}}(\tau) = \frac{\exp\left(-\frac{\left(\log(t) - \log\left(\frac{m^2}{\sqrt{m^2+v}}\right)\right)^2}{2 \log\left(\frac{v}{m^2} + 1\right)}\right)}{\sqrt{2\pi t} \sqrt{\log\left(\frac{v}{m^2} + 1\right)}}, \quad m = 5, v = 3; \quad (65)$$

TABLE II: Comparison of the properties of all the considered real-world networks.

Network	$N$	$r$	$\bar{c}$	$m_1$	$\bar{k}$	$R_0$	$R$	$R_{\text{pert}}$	Error
amazon	$2.6 \times 10^5$	-0.0	0.4	2.4	6.9	10.1	7.9	7.6	0.03
asCaida	$2.6 \times 10^4$	-0.19	0.2	2.0	4.0	279.2	43.6	23.0	0.47
asOregon	$1.1 \times 10^4$	-0.19	0.3	2.3	4.1	251.2	31.3	13.8	0.56
astroPh	$1.9 \times 10^4$	0.21	0.6	20.5	21.1	64.4	52.5	58.9	0.12
brightkite	$5.8 \times 10^4$	0.01	0.2	6.9	7.4	62.7	53.4	58.8	0.1
condMat	$2.3 \times 10^4$	0.14	0.6	5.6	8.1	21.1	19.7	21.4	0.09
DBLP	$3.2 \times 10^5$	0.27	0.6	6.4	6.6	20.7	18.3	23.1	0.26
deezerEurope	$2.8 \times 10^4$	0.1	0.1	1.5	6.6	15.2	15.5	15.7	0.01
deezerHR	$5.5 \times 10^4$	0.2	0.1	4.0	18.3	34.9	36.1	36.2	0.01
deezerHU	$4.8 \times 10^4$	0.21	0.1	1.3	9.4	14.2	14.6	14.5	0.01
deezerRO	$4.2 \times 10^4$	0.11	0.1	0.8	6.0	10.1	10.3	10.4	0.01
douban	$1.5 \times 10^5$	-0.18	0.0	0.4	4.2	35.9	32.0	29.4	0.08
email	$3.7 \times 10^4$	-0.11	0.5	11.9	10.0	139.1	83.5	76.0	0.09
fbArtist	$5.1 \times 10^4$	-0.02	0.1	8.3	32.4	155.7	142.4	141.4	0.01
fbAthletes	$1.4 \times 10^4$	-0.03	0.3	4.9	12.5	37.4	30.5	30.5	0.0
fbCompany	$1.4 \times 10^4$	0.01	0.2	3.3	7.4	21.0	18.1	18.4	0.02
fbNewSites	$2.8 \times 10^4$	0.02	0.3	5.7	14.8	49.5	47.4	47.0	0.01
fbPublicFigures	$1.2 \times 10^4$	0.2	0.2	8.3	11.6	49.6	51.6	54.2	0.05
github	$3.8 \times 10^4$	-0.08	0.2	5.4	15.3	440.0	106.9	62.8	0.41
gowalla	$2.0 \times 10^5$	-0.03	0.2	7.2	9.7	305.6	115.2	64.1	0.44
hamsterster	$9.2 \times 10^2$	-0.12	0.2	4.3	8.8	32.9	22.2	24.2	0.09
internet	$2.3 \times 10^4$	-0.2	0.2	2.9	4.2	260.5	44.8	23.4	0.48
lastfm	$7.6 \times 10^3$	0.02	0.2	4.4	7.3	24.4	17.7	20.8	0.17
livemocha	$1.0 \times 10^5$	-0.15	0.1	4.6	42.1	326.6	251.2	233.8	0.07
museaFacebook	$2.2 \times 10^4$	0.09	0.4	14.0	15.2	60.1	50.2	58.4	0.16
pgp	$1.1 \times 10^4$	0.24	0.3	6.8	4.6	17.9	12.9	19.0	0.47
PIN	$1.9 \times 10^3$	-0.16	0.1	0.7	2.4	5.5	3.8	3.0	0.22
powergrid	$4.9 \times 10^3$	0.0	0.1	0.3	2.7	2.9	2.5	2.6	0.02
roadCA	$2.0 \times 10^6$	0.13	0.0	0.1	2.8	2.2	2.1	2.1	0.02
roadPA	$1.1 \times 10^6$	0.12	0.0	0.1	2.8	2.2	2.1	2.1	0.0
roadTX	$1.4 \times 10^6$	0.13	0.0	0.1	2.8	2.1	2.1	2.1	0.03
wordnet	$1.5 \times 10^5$	-0.06	0.6	5.2	9.0	54.6	37.8	29.9	0.21

and a Weibull distribution with scale 2 and shape 2:

$$\psi_{\text{wei}}(\tau) = \frac{1}{2} e^{-\frac{\tau^2}{4}} \tau. \quad (66)$$

The epidemic starts with one infected individual, chosen uniformly at random. To simulate the epidemics, we implemented a next reaction scheme [13].

#### D. Power-law fit of the trajectories

The fitting procedure of a generalised logistic function described in Methods fails for epidemics on the California, Pennsylvania, and Texas road networks [10]. Instead, their behaviour appears more similar to a power-law  $I(t) \propto t^\beta$ . We therefore fit a power-law to three US road networks, the US powergrid, and compare it to the Condensed Matter citation network, that has a clear exponential phase, see Fig. 5. The power-law fits are excellent for the US road networks, while the generalised logistic function provides a better fit for the US powergrid network. This supports that finite-size effects ( $\eta = 0.497$ ) are more likely to explain the deviation from the predicted spreading rate for the powergrid network ( $\Lambda_{\text{EL}} = 0.196$  versus  $\Lambda_{\text{FIT}} = 0.351$ ) rather than the presence of a power-law behaviour.

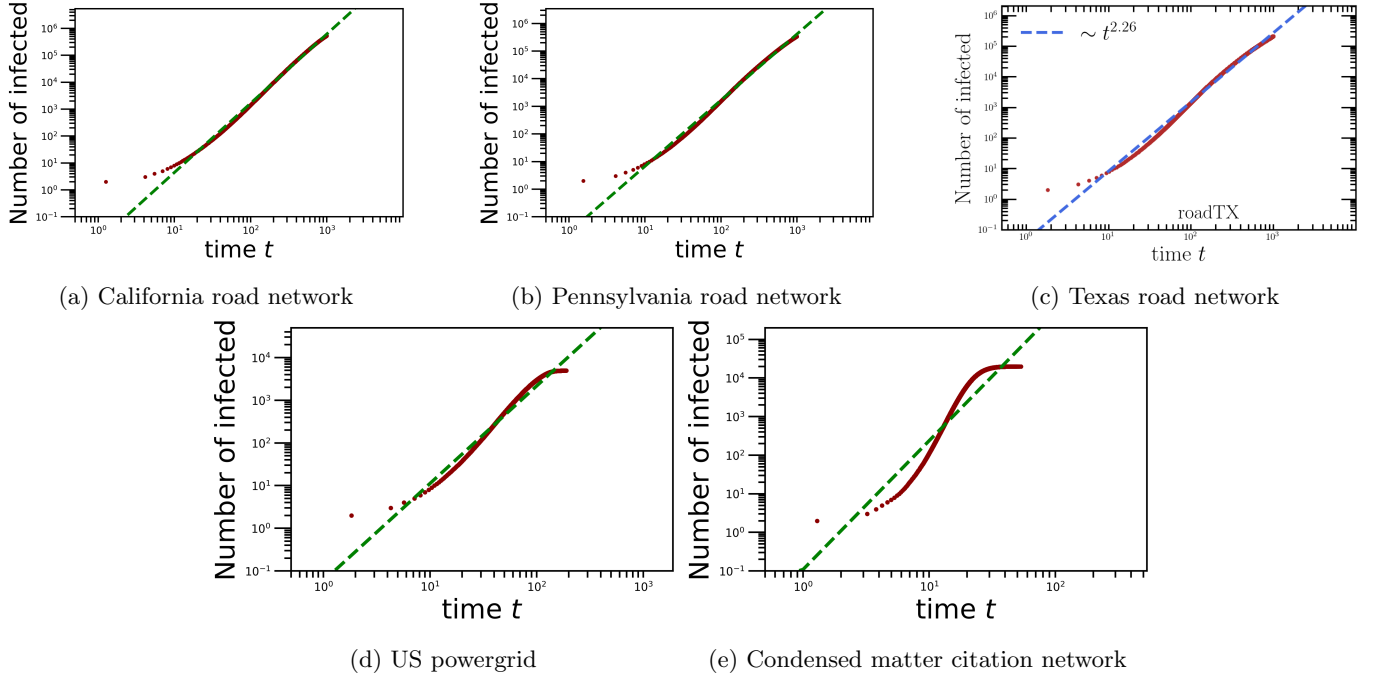


FIG. 5: **Comparison between power-law fit and generalised logistic fit for road networks.** We plot the average epidemic trajectories (red dots) for the three road networks (panels (a)-(b)-(c)), the US powergrid (d) and the condensed matter citation network (e). We fit a power-law (blue) and the generalised logistic function (black) for each trajectory. The infection times are lognormally distributed, see Eq. (64).

## E. Trajectories Synthetic Networks

### 1. Gamma

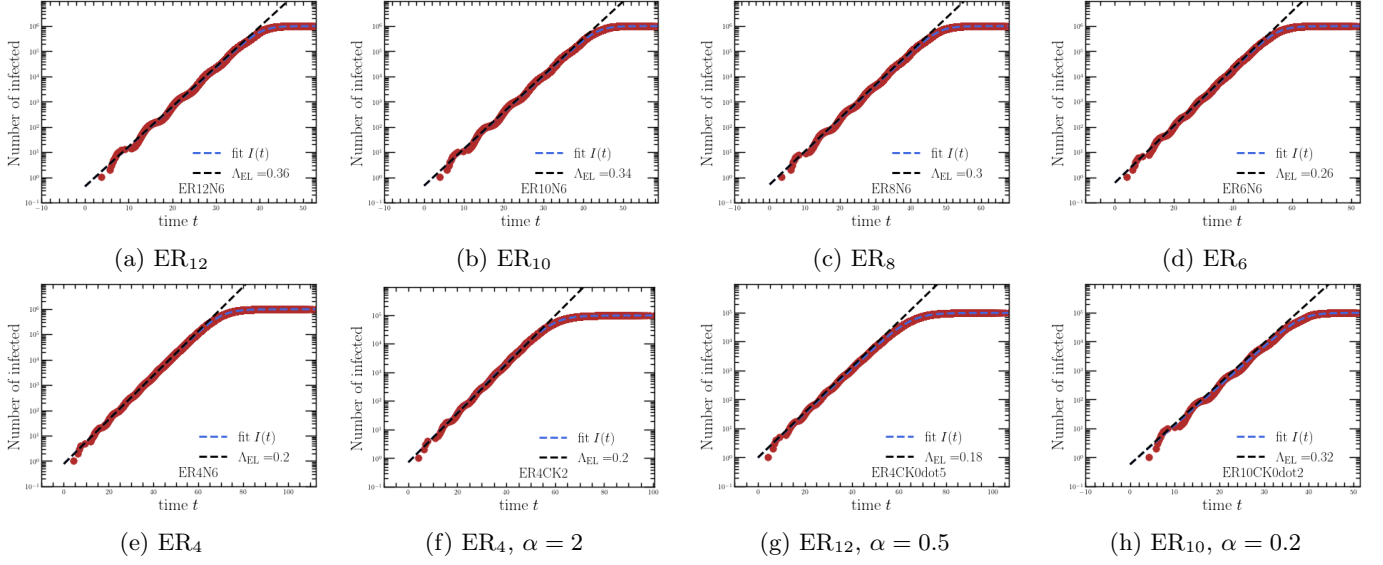


FIG. 6: Average epidemic trajectories on Erdős-Rényi networks with a Lognormal generation-time distribution.

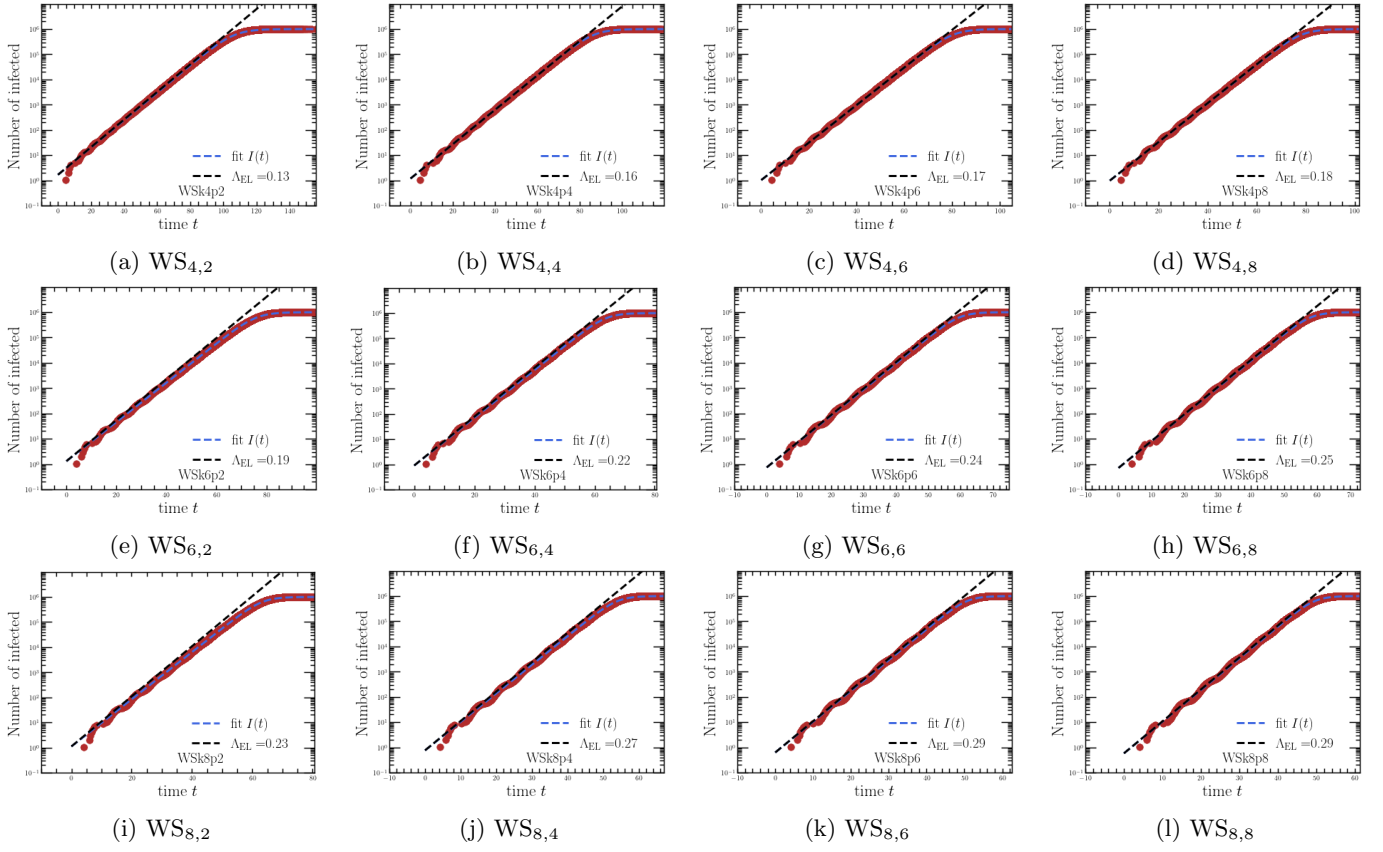


FIG. 7: Average epidemic trajectories on Watts–Strogatz networks with a Lognormal generation-time distribution.

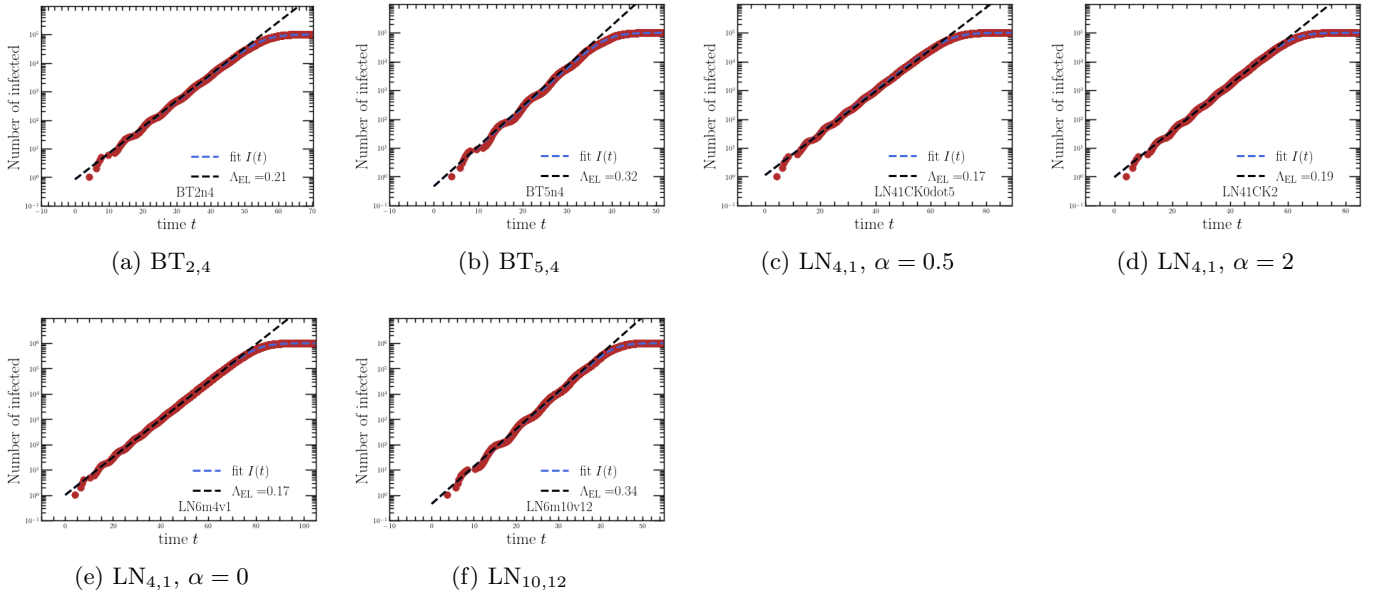


FIG. 8: Average epidemic trajectories on networks from the configuration model with a Gamma generation-time distribution.

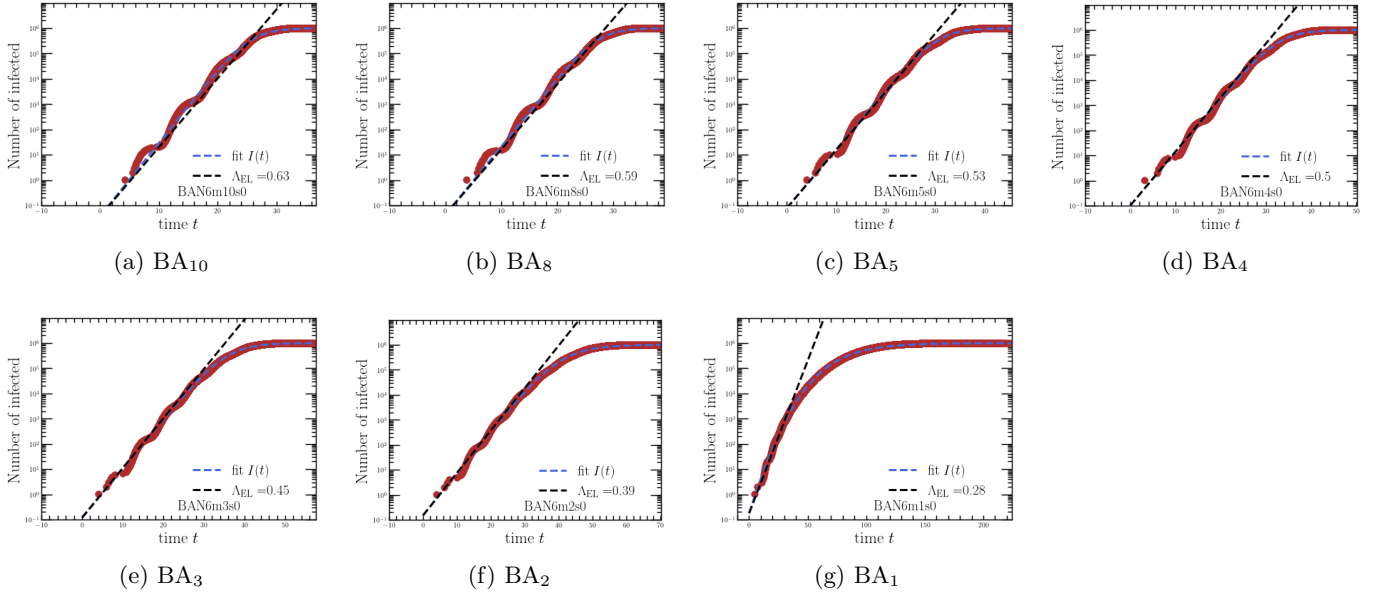


FIG. 9: Average epidemic trajectories on Barabási-Albert networks with a Gamma generation-time distribution.

TABLE III: Results of the fitting procedure for synthetic networks with a Gamma generation-time distribution

Network	$\Lambda_{\text{FIT}}$	$\Lambda_R$	Error $_R$	$\Lambda_{R_{\text{pert}}}$	Error $_{R_{\text{pert}}}$	$\Lambda_{R_0}$	Error $_{R_0}$	$\Lambda_0$	$I_{0(\text{fit})}$	$\nu$
BA <sub>1</sub>	0.33	0.31	-0.05	0.28	-0.17	0.39	0.16	0.44	0.18	0.09
BA <sub>2</sub>	0.39	0.4	0.03	0.39	0.0	0.44	0.13	0.39	0.15	0.45
BA <sub>3</sub>	0.45	0.46	0.02	0.45	0.01	0.49	0.09	0.45	0.12	0.55
BA <sub>4</sub>	0.49	0.5	0.02	0.5	0.01	0.52	0.07	0.49	0.1	0.61
BA <sub>5</sub>	0.54	0.53	-0.01	0.53	-0.02	0.55	0.03	0.54	0.08	0.62
BA <sub>8</sub>	0.62	0.6	-0.04	0.59	-0.05	0.61	-0.02	0.62	0.04	0.65
BA <sub>10</sub>	0.67	0.63	-0.06	0.63	-0.06	0.64	-0.04	0.67	0.04	0.62
BA <sub>12</sub>	0.68	0.66	-0.04	0.65	-0.05	0.67	-0.03	0.68	0.04	0.68
ER <sub>4</sub>	0.2	0.2	0.0	0.2	0.0	0.2	0.0	0.2	0.77	1.12
ER <sub>6</sub>	0.26	0.26	0.01	0.26	0.01	0.26	0.01	0.26	0.61	1.28
ER <sub>8</sub>	0.3	0.3	0.01	0.3	0.01	0.3	0.01	0.3	0.52	1.37
ER <sub>10</sub>	0.33	0.34	0.01	0.34	0.01	0.34	0.01	0.33	0.46	1.42
ER <sub>12</sub>	0.36	0.36	0.01	0.36	0.01	0.36	0.01	0.36	0.43	1.47
ER <sub>10</sub> $\alpha = 0.2$	0.31	0.32	0.03	0.32	0.03	0.34	0.08	0.31	0.57	1.47
ER <sub>4</sub> $\alpha = 2$	0.2	0.2	0.0	0.2	-0.01	0.2	0.01	0.2	0.71	1.09
ER <sub>4</sub> $\alpha = 0.5$	0.18	0.18	0.01	0.18	0.02	0.2	0.13	0.18	0.98	1.1
LN <sub>4,1</sub> $\alpha = 0.5$	0.17	0.17	-0.02	0.17	-0.01	0.19	0.12	0.17	1.13	1.42
LN <sub>4,1</sub> $\alpha = 2$	0.19	0.19	-0.0	0.19	-0.0	0.19	0.03	0.19	0.96	1.44
BT <sub>2,4</sub>	0.21	0.21	0.01	0.21	0.01	0.21	0.01	0.21	0.84	1.48
BT <sub>5,4</sub>	0.32	0.32	0.02	0.32	0.02	0.32	0.02	0.32	0.46	1.3
LN <sub>10,12</sub>	0.34	0.34	0.01	0.34	0.01	0.34	0.01	0.34	0.45	1.41
LN <sub>4,1</sub>	0.17	0.17	-0.0	0.17	-0.0	0.17	-0.0	0.17	1.01	1.35
WS <sub>4,2</sub>	0.13	0.13	0.01	0.13	0.01	0.17	0.29	0.13	1.65	1.23
WS <sub>4,4</sub>	0.16	0.16	-0.0	0.16	-0.0	0.17	0.1	0.16	1.17	1.31
WS <sub>4,6</sub>	0.17	0.17	0.0	0.17	0.0	0.18	0.04	0.17	1.02	1.34
WS <sub>4,8</sub>	0.18	0.18	0.0	0.18	0.0	0.18	0.02	0.18	0.97	1.34
WS <sub>6,2</sub>	0.18	0.19	0.05	0.19	0.05	0.24	0.29	0.18	1.3	1.37
WS <sub>6,4</sub>	0.22	0.22	0.02	0.22	0.02	0.24	0.11	0.22	0.89	1.47
WS <sub>6,6</sub>	0.24	0.24	0.01	0.24	0.01	0.25	0.04	0.24	0.74	1.47
WS <sub>6,8</sub>	0.24	0.25	0.01	0.25	0.01	0.25	0.01	0.24	0.7	1.47
WS <sub>8,2</sub>	0.22	0.23	0.06	0.23	0.06	0.29	0.28	0.22	1.1	1.49
WS <sub>8,4</sub>	0.26	0.27	0.03	0.27	0.03	0.29	0.11	0.26	0.75	1.52
WS <sub>8,6</sub>	0.28	0.29	0.01	0.29	0.01	0.29	0.04	0.28	0.62	1.53
WS <sub>8,8</sub>	0.29	0.29	0.01	0.29	0.01	0.29	0.01	0.29	0.58	1.52

## 2. Lognormal

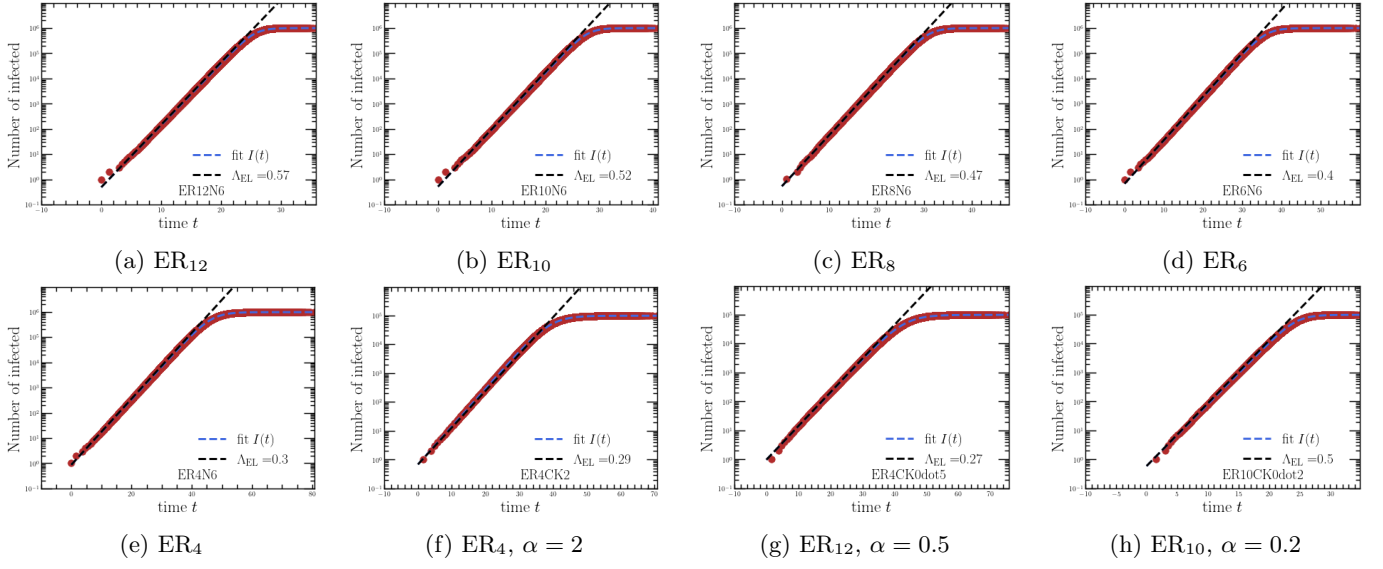


FIG. 10: Average epidemic trajectories on Erdős-Rényi networks from the configuration model with a Lognormal generation-time distribution.

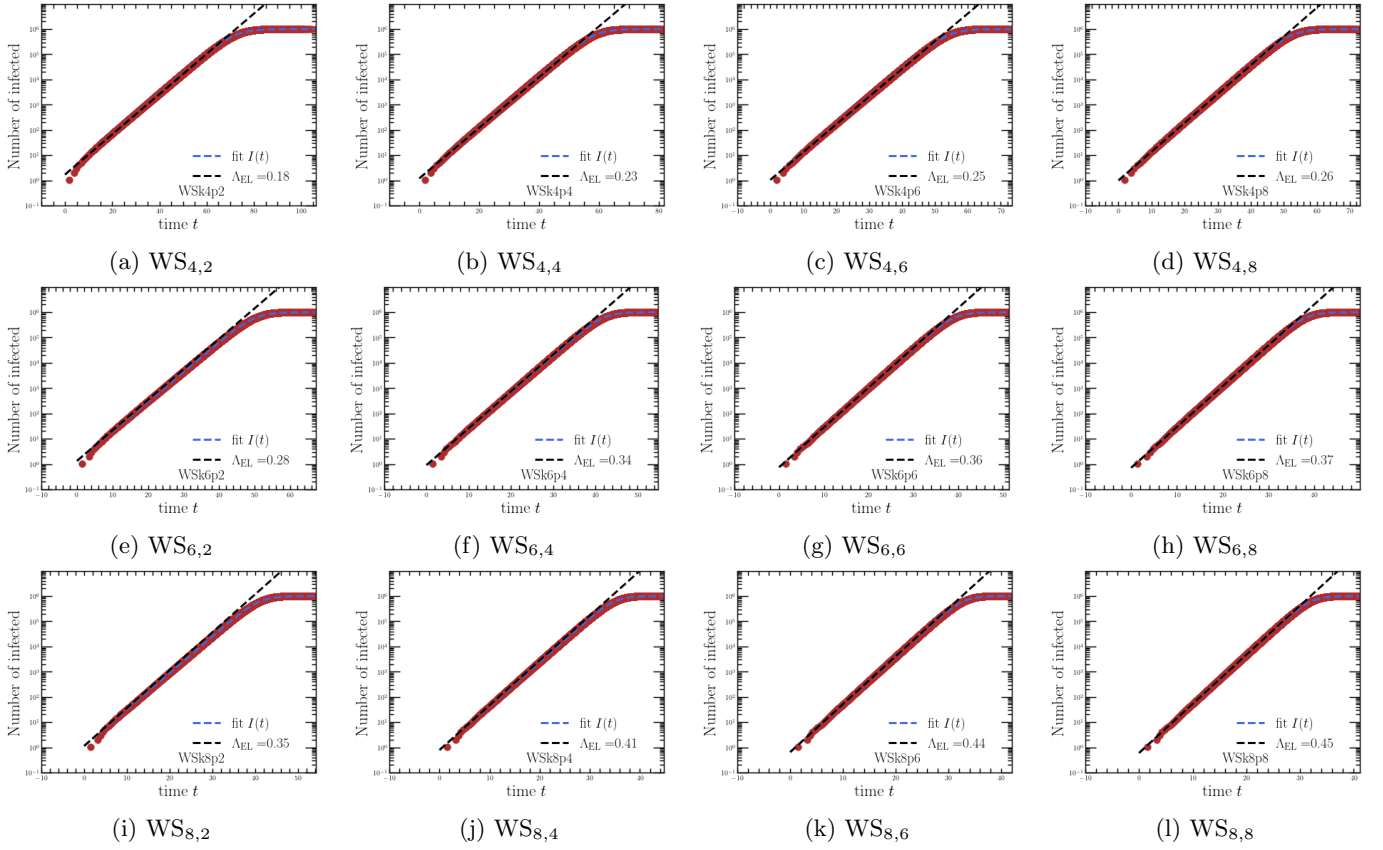


FIG. 11: Average epidemic trajectories on Watts–Strogatz networks with a Lognormal generation-time distribution.

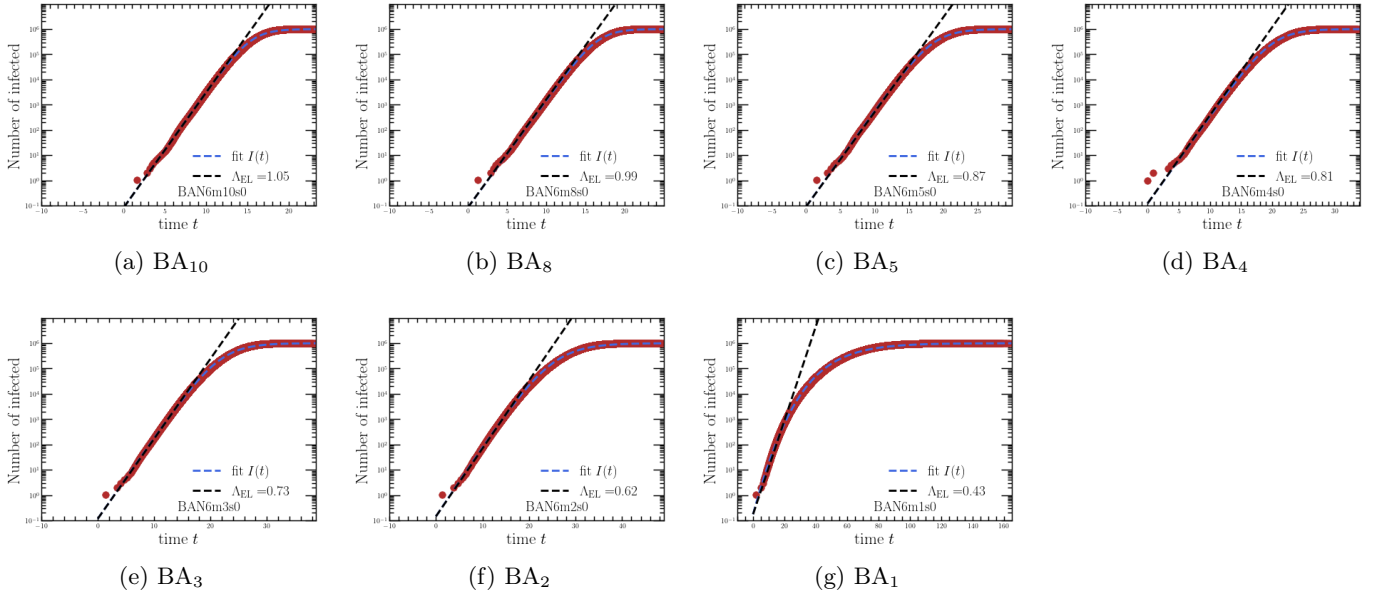


FIG. 12: Average epidemic trajectories on Barabási-Albert networks with a Lognormal generation-time distribution.

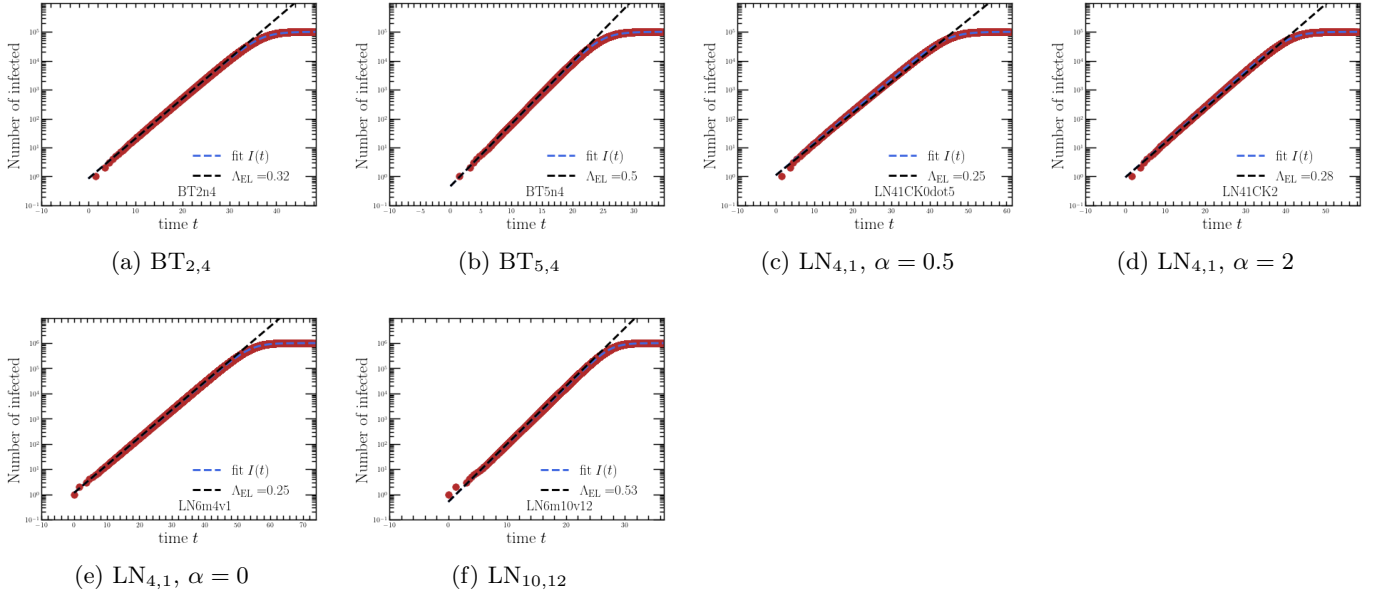


FIG. 13: Average epidemic trajectories on networks from the configuration model with a Lognormal generation-time distribution.

TABLE IV: Results of the fitting procedure for synthetic networks with a Lognormal generation-time distribution

Network	$\Lambda_{\text{FIT}}$	$\Lambda_R$	Error $_R$	$\Lambda_{R_{\text{pert}}}$	Error $_{R_{\text{pert}}}$	$\Lambda_{R_0}$	Error $_{R_0}$	$\Lambda_0$	$I_{0(\text{fit})}$	$\nu$
BA <sub>1</sub>	0.52	0.48	-0.07	0.43	-0.2	0.61	0.16	0.87	0.17	0.06
BA <sub>2</sub>	0.63	0.64	0.01	0.62	-0.02	0.71	0.12	0.63	0.14	0.37
BA <sub>3</sub>	0.74	0.74	0.0	0.73	-0.01	0.8	0.08	0.74	0.12	0.45
BA <sub>4</sub>	0.8	0.81	0.02	0.81	0.01	0.86	0.08	0.8	0.12	0.51
BA <sub>5</sub>	0.88	0.87	-0.01	0.87	-0.01	0.91	0.03	0.88	0.09	0.54
BA <sub>8</sub>	0.98	0.99	0.01	0.99	0.01	1.01	0.03	0.98	0.08	0.67
BA <sub>10</sub>	1.06	1.06	0.0	1.05	-0.0	1.08	0.02	1.06	0.08	0.65
BA <sub>12</sub>	1.1	1.11	0.01	1.11	0.0	1.13	0.02	1.1	0.09	0.69
ER <sub>4</sub>	0.3	0.3	0.01	0.3	0.01	0.3	0.01	0.3	0.87	1.08
ER <sub>6</sub>	0.39	0.4	0.01	0.4	0.01	0.4	0.01	0.39	0.67	1.21
ER <sub>8</sub>	0.47	0.47	0.0	0.47	0.0	0.47	0.0	0.47	0.53	1.22
ER <sub>10</sub>	0.52	0.52	0.01	0.52	0.01	0.52	0.01	0.52	0.51	1.32
ER <sub>12</sub>	0.57	0.57	0.01	0.57	0.01	0.57	0.01	0.57	0.48	1.38
ER <sub>10</sub> $\alpha = 0.2$	0.49	0.5	0.01	0.5	0.02	0.52	0.07	0.49	0.59	1.32
ER <sub>4</sub> $\alpha = 2$	0.3	0.3	-0.01	0.29	-0.03	0.3	-0.0	0.3	0.68	0.97
ER <sub>4</sub> $\alpha = 0.5$	0.27	0.26	-0.01	0.27	0.01	0.3	0.12	0.27	0.97	0.99
LN <sub>4,1</sub> $\alpha = 0.5$	0.25	0.25	-0.04	0.25	-0.03	0.29	0.11	0.25	1.1	1.28
LN <sub>4,1</sub> $\alpha = 2$	0.28	0.28	-0.02	0.28	-0.02	0.29	0.01	0.28	0.93	1.27
BT <sub>2,4</sub>	0.32	0.32	0.0	0.32	0.0	0.32	0.0	0.32	0.84	1.33
BT <sub>5,4</sub>	0.49	0.5	0.01	0.5	0.0	0.5	0.0	0.49	0.46	1.13
LN <sub>10,12</sub>	0.53	0.53	0.01	0.53	0.01	0.53	0.01	0.53	0.5	1.31
LN <sub>4,1</sub>	0.25	0.25	0.0	0.25	0.0	0.25	0.0	0.25	1.14	1.35
WS <sub>4,2</sub>	0.18	0.18	0.0	0.18	-0.01	0.25	0.29	0.18	1.69	1.18
WS <sub>4,4</sub>	0.23	0.23	-0.01	0.23	-0.01	0.26	0.1	0.23	1.19	1.23
WS <sub>4,6</sub>	0.25	0.25	-0.0	0.25	-0.0	0.26	0.04	0.25	1.04	1.25
WS <sub>4,8</sub>	0.26	0.26	-0.0	0.26	-0.0	0.27	0.02	0.26	0.99	1.24
WS <sub>6,2</sub>	0.27	0.28	0.03	0.28	0.03	0.36	0.29	0.27	1.33	1.29
WS <sub>6,4</sub>	0.33	0.34	0.01	0.34	0.01	0.37	0.1	0.33	0.91	1.35
WS <sub>6,6</sub>	0.36	0.36	0.0	0.36	0.0	0.37	0.03	0.36	0.75	1.34
WS <sub>6,8</sub>	0.37	0.37	0.0	0.37	0.0	0.38	0.01	0.37	0.71	1.33
WS <sub>8,2</sub>	0.33	0.35	0.04	0.35	0.04	0.44	0.28	0.33	1.13	1.39
WS <sub>8,4</sub>	0.4	0.41	0.02	0.41	0.02	0.44	0.1	0.4	0.78	1.39
WS <sub>8,6</sub>	0.43	0.44	0.01	0.44	0.01	0.45	0.03	0.43	0.64	1.39
WS <sub>8,8</sub>	0.45	0.45	0.0	0.45	0.0	0.45	0.01	0.45	0.6	1.38

3. Weibull

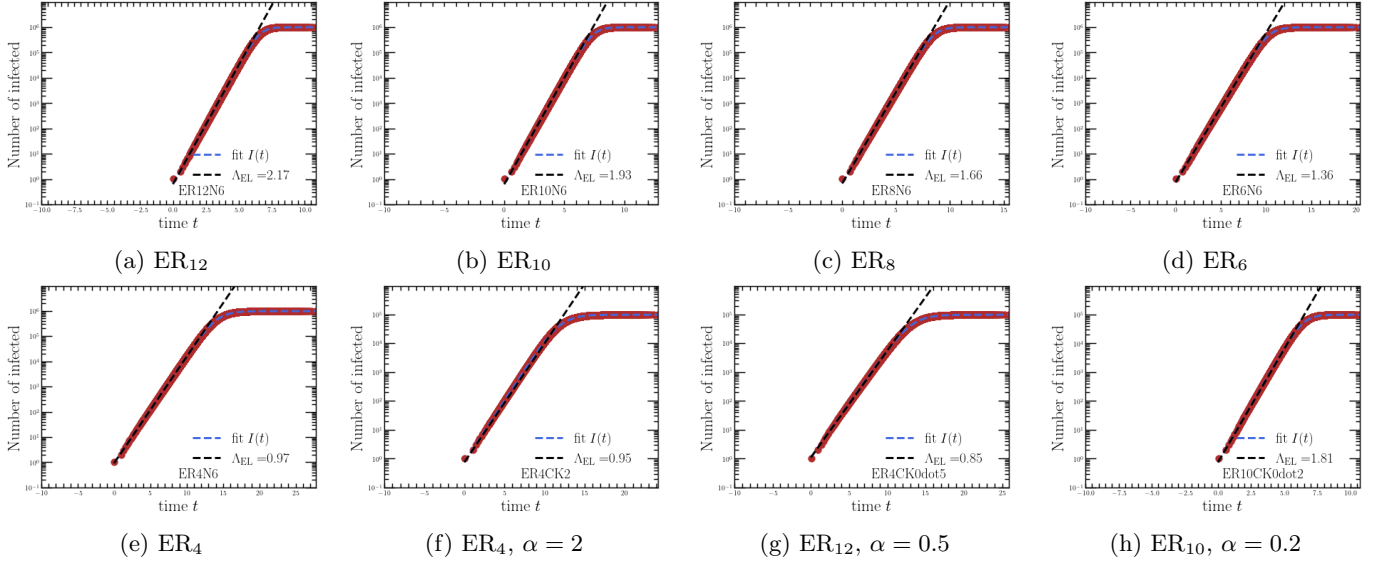


FIG. 14: Average epidemic trajectories on Erdős-Rényi networks with a Weibull generation-time distribution.

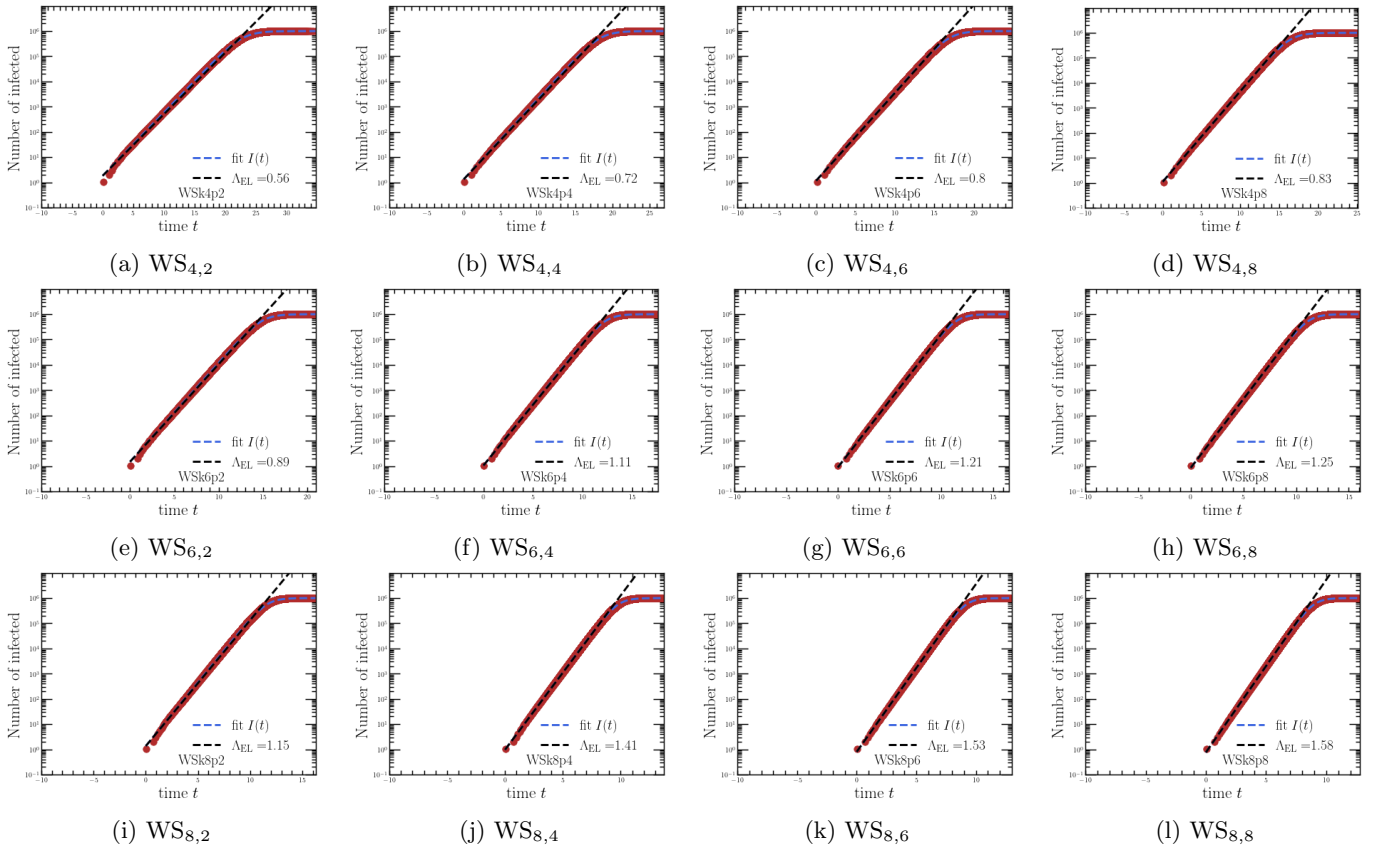


FIG. 15: Average epidemic trajectories on Watts–Strogatz networks with a Weibull generation-time distribution.

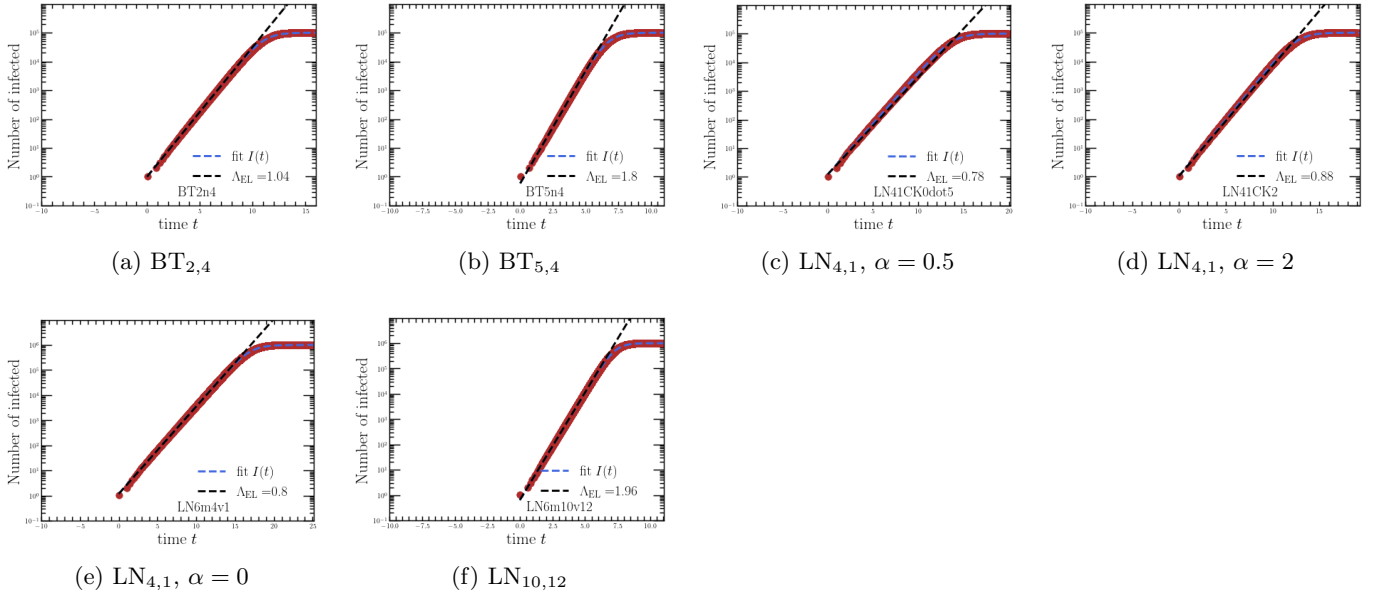


FIG. 16: Average epidemic trajectories on networks from the configuration model with a Weibull generation-time distribution.

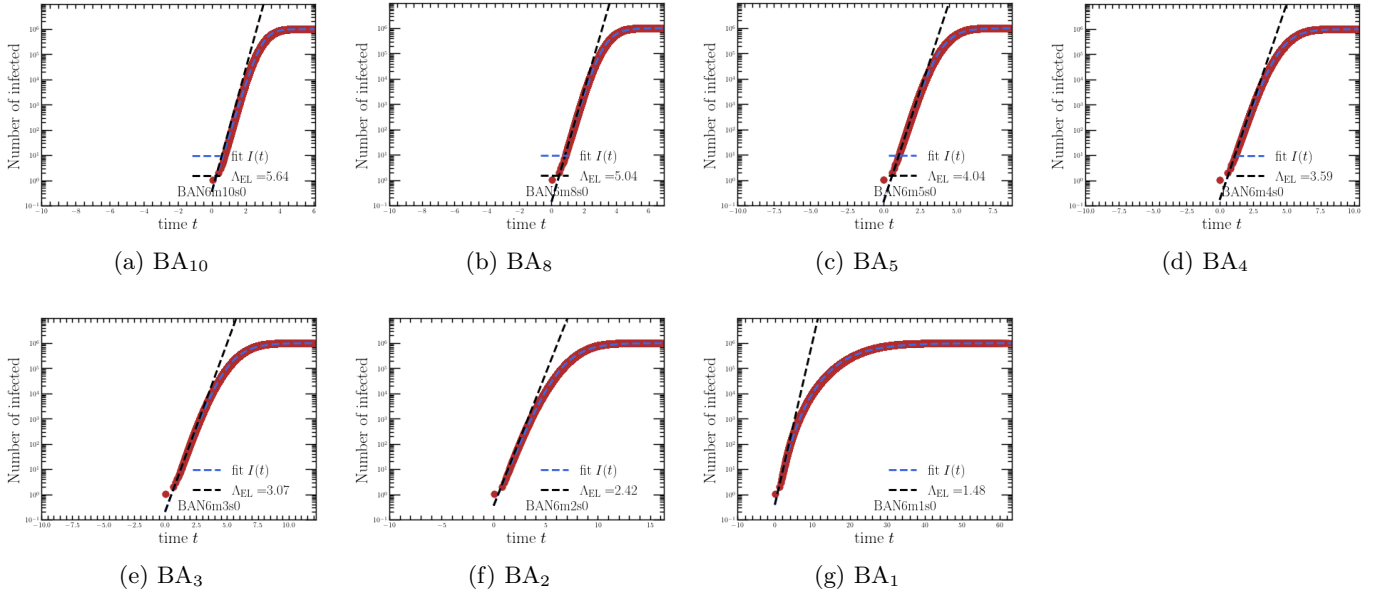


FIG. 17: Average epidemic trajectories on Barabási-Albert networks from the configuration model with a Weibull generation-time distribution.

TABLE V: Results of the fitting procedure for synthetic networks with a Weibull generation-time distribution

Network	$\Lambda_{\text{FIT}}$	$\Lambda_R$	Error $_R$	$\Lambda_{R_{\text{pert}}}$	Error $_{R_{\text{pert}}}$	$\Lambda_{R_0}$	Error $_{R_0}$	$\Lambda_0$	$I_{0(\text{fit})}$	$\nu$
BA <sub>1</sub>	1.6	1.74	0.08	1.48	-0.08	2.37	0.39	5.0	0.38	0.03
BA <sub>2</sub>	2.31	2.53	0.09	2.42	0.05	2.97	0.25	2.35	0.35	0.27
BA <sub>3</sub>	3.1	3.15	0.02	3.07	-0.01	3.54	0.13	3.14	0.2	0.28
BA <sub>4</sub>	3.54	3.65	0.03	3.59	0.01	3.98	0.12	3.57	0.17	0.31
BA <sub>5</sub>	4.1	4.07	-0.01	4.04	-0.01	4.36	0.06	4.12	0.13	0.32
BA <sub>8</sub>	4.98	5.08	0.02	5.04	0.01	5.27	0.06	5.0	0.14	0.36
BA <sub>10</sub>	5.0	5.69	0.13	5.64	0.12	5.88	0.16	5.0	0.35	0.52
ER <sub>4</sub>	0.98	0.97	-0.01	0.97	-0.01	0.97	-0.01	0.98	0.92	0.88
ER <sub>6</sub>	1.36	1.36	-0.0	1.36	-0.0	1.36	-0.0	1.36	0.76	0.97
ER <sub>8</sub>	1.67	1.66	-0.0	1.66	-0.0	1.66	-0.0	1.67	0.67	1.0
ER <sub>10</sub>	1.93	1.93	0.0	1.93	0.0	1.93	0.0	1.93	0.63	1.02
ER <sub>12</sub>	2.16	2.17	0.0	2.17	0.0	2.17	0.0	2.16	0.63	1.07
ER <sub>10</sub> $\alpha = 0.2$	1.83	1.8	-0.02	1.81	-0.01	1.93	0.06	1.83	0.75	1.06
ER <sub>4</sub> $\alpha = 2$	0.98	0.96	-0.02	0.95	-0.04	0.97	-0.01	0.98	0.75	0.83
ER <sub>4</sub> $\alpha = 0.5$	0.86	0.84	-0.03	0.85	-0.01	0.97	0.12	0.86	1.1	0.85
LN <sub>4,1</sub> $\alpha = 0.5$	0.82	0.77	-0.05	0.78	-0.05	0.91	0.11	0.82	1.23	1.13
LN <sub>4,1</sub> $\alpha = 2$	0.9	0.88	-0.02	0.88	-0.03	0.91	0.01	0.9	1.05	1.09
BT <sub>2,4</sub>	1.04	1.04	-0.0	1.04	-0.0	1.04	-0.0	1.04	0.99	1.13
BT <sub>5,4</sub>	1.8	1.81	0.0	1.8	0.0	1.8	0.0	1.8	0.59	0.88
LN <sub>10,12</sub>	1.96	1.96	0.0	1.96	0.0	1.96	0.0	1.96	0.64	1.01
LN <sub>4,1</sub>	0.81	0.8	-0.01	0.8	-0.01	0.8	-0.01	0.81	1.17	1.11
WS <sub>4,2</sub>	0.58	0.56	-0.03	0.56	-0.03	0.78	0.3	0.58	1.81	1.1
WS <sub>4,4</sub>	0.74	0.72	-0.02	0.72	-0.02	0.81	0.1	0.74	1.31	1.1
WS <sub>4,6</sub>	0.81	0.8	-0.01	0.8	-0.01	0.84	0.04	0.81	1.16	1.1
WS <sub>4,8</sub>	0.84	0.83	-0.0	0.83	-0.0	0.85	0.02	0.84	1.1	1.08
WS <sub>6,2</sub>	0.9	0.89	-0.01	0.89	-0.01	1.21	0.29	0.9	1.48	1.15
WS <sub>6,4</sub>	1.11	1.11	-0.01	1.11	-0.01	1.23	0.1	1.11	1.05	1.16
WS <sub>6,6</sub>	1.21	1.21	-0.0	1.21	-0.0	1.25	0.03	1.21	0.88	1.13
WS <sub>6,8</sub>	1.25	1.25	0.0	1.25	0.0	1.26	0.01	1.25	0.85	1.13
WS <sub>8,2</sub>	1.16	1.15	-0.01	1.15	-0.01	1.54	0.28	1.16	1.34	1.2
WS <sub>8,4</sub>	1.42	1.41	-0.01	1.41	-0.0	1.56	0.1	1.42	0.96	1.17
WS <sub>8,6</sub>	1.53	1.53	-0.0	1.53	0.0	1.58	0.03	1.53	0.79	1.15
WS <sub>8,8</sub>	1.58	1.58	0.0	1.58	0.0	1.59	0.01	1.58	0.75	1.13

## F. Trajectories real networks

### 1. Lognormal

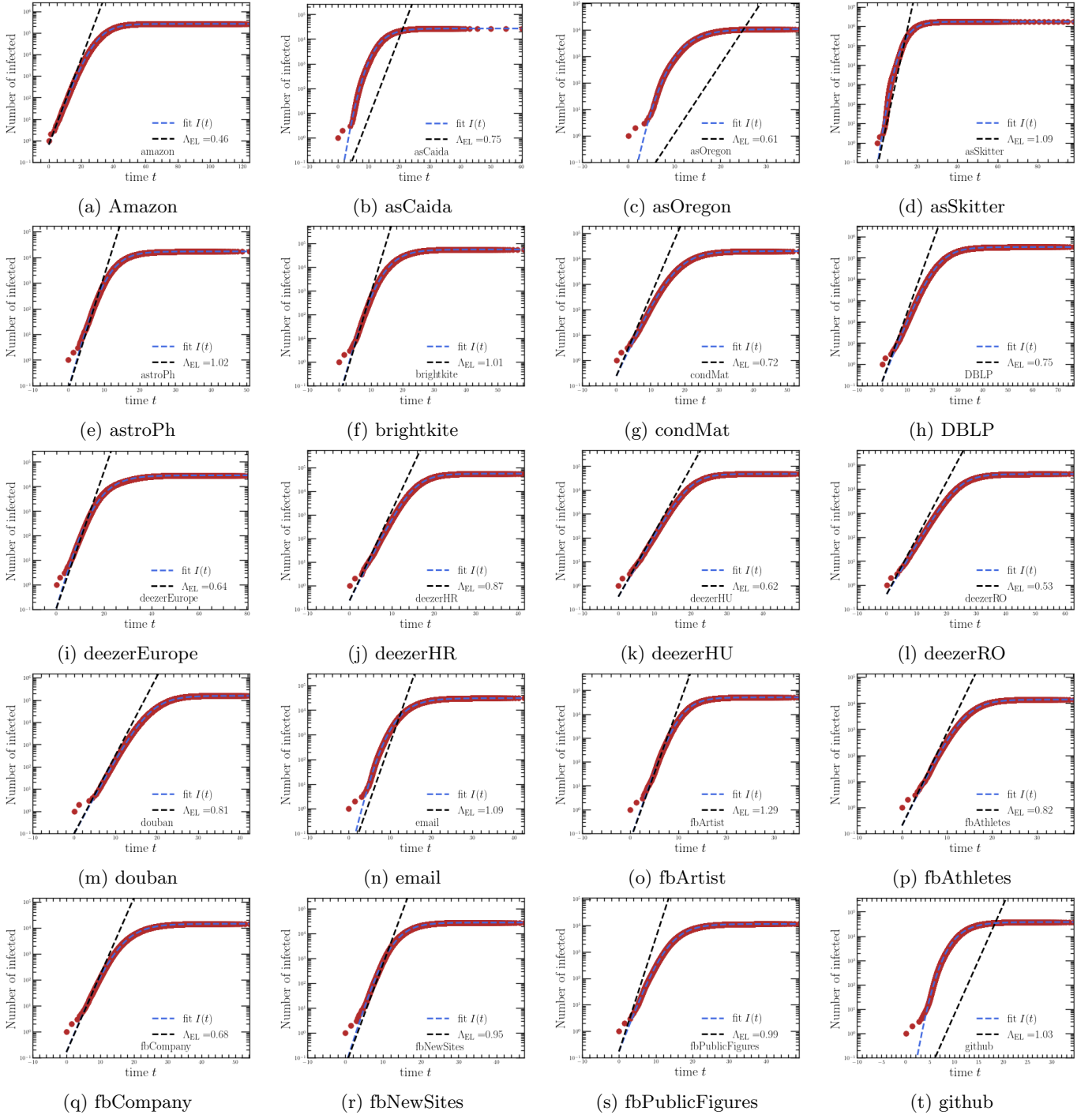


FIG. 18: Average epidemic trajectories on real-world networks with a Lognormal generation-time distribution (I).

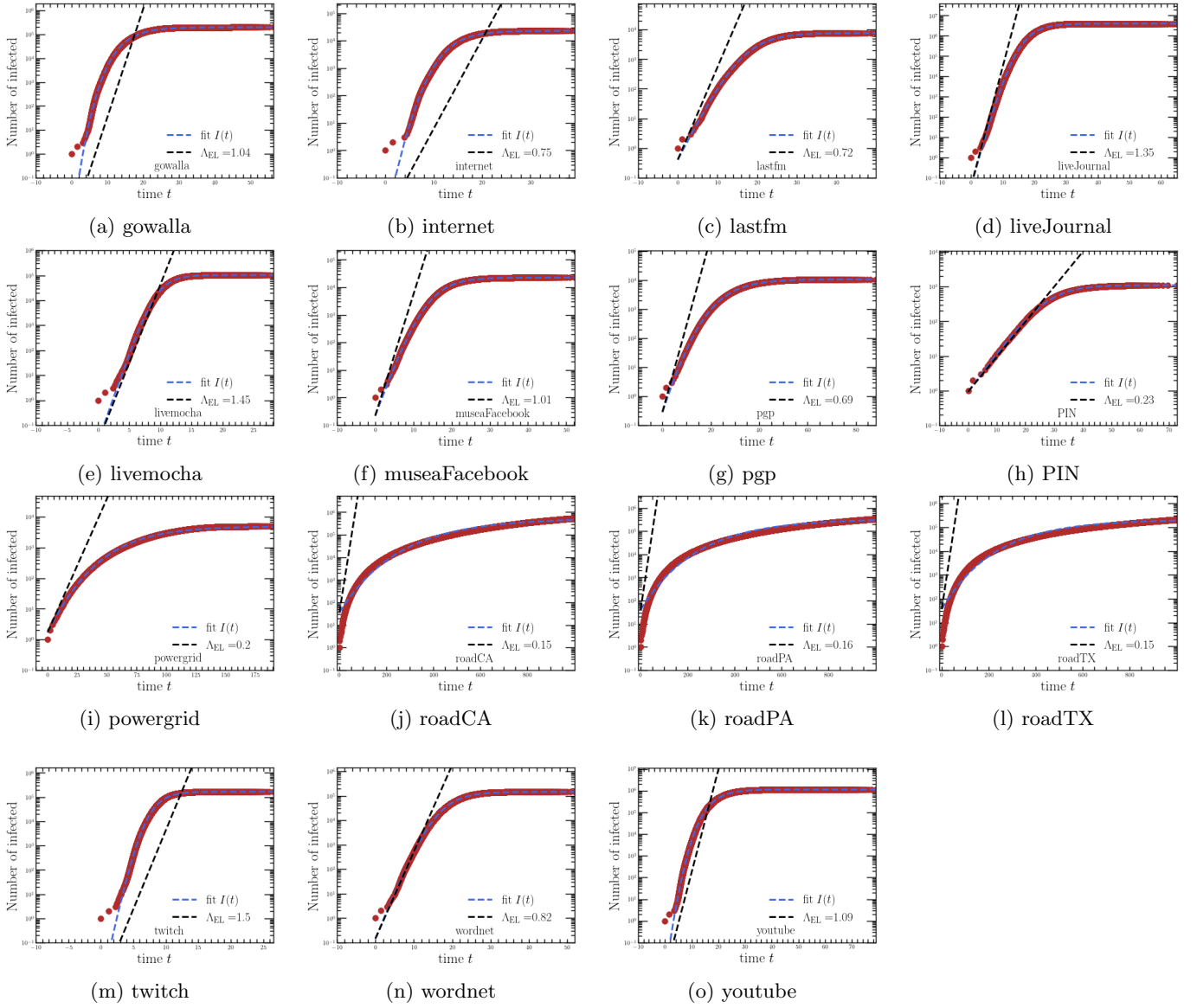


FIG. 19: Average epidemic trajectories on real-world networks with a Lognormal generation-time distribution (II).

TABLE VI: Results and parameters from the fitting procedure on real-world networks with a Lognormal generation-time distribution.

Network	$\Lambda_{FIT}$	$\Lambda_R$	Error $_R$	$\Lambda_{R_{pert}}$	Error $_{R_{pert}}$	$\Lambda_{R_0}$	Error $_{R_0}$	$\Lambda_0$	$I_{0(fit)}$	$\nu$	$\eta$
amazon	0.44	0.46	0.04	0.46	0.02	0.53	0.17	0.45	0.64	0.33	0.01
asCaida	1.74	0.93	-0.61	0.75	-0.8	1.51	-0.14	2.0	0.0	0.13	0.13
asOregon	1.88	0.83	-0.78	0.61	-1.03	1.47	-0.24	2.29	0.0	0.11	0.18
asSkitter	1.64	1.55	-0.06	1.09	-0.4	2.1	0.25	1.87	0.05	0.12	0.12
astroPh	1.15	0.98	-0.15	1.02	-0.12	1.04	-0.09	1.2	0.07	0.25	0.05
brightkite	1.11	0.99	-0.12	1.01	-0.09	1.03	-0.07	1.18	0.03	0.2	0.05
condMat	0.65	0.7	0.08	0.72	0.11	0.72	0.11	0.66	0.24	0.36	0.02
DBLP	0.66	0.68	0.03	0.75	0.12	0.72	0.08	0.67	0.16	0.32	0.01
deezerEurope	0.76	0.64	-0.17	0.64	-0.17	0.63	-0.18	0.83	0.11	0.19	0.09
deezerHR	0.81	0.87	0.07	0.87	0.07	0.86	0.06	0.82	0.23	0.45	0.0
deezerHU	0.59	0.62	0.05	0.62	0.05	0.61	0.04	0.59	0.33	0.57	0.0
deezerRO	0.48	0.53	0.11	0.53	0.12	0.53	0.1	0.48	0.43	0.55	0.0
douban	0.78	0.84	0.08	0.81	0.05	0.87	0.11	0.78	0.1	0.4	0.0
email	1.6	1.12	-0.35	1.09	-0.38	1.28	-0.22	1.76	0.01	0.16	0.09
fbArtist	1.36	1.29	-0.06	1.29	-0.06	1.32	-0.03	1.38	0.05	0.31	0.01
fbAthletes	0.8	0.82	0.03	0.82	0.03	0.88	0.1	0.8	0.2	0.43	0.01
fbCompany	0.72	0.68	-0.05	0.68	-0.05	0.72	0.01	0.74	0.16	0.3	0.03
fbNewSites	1.11	0.95	-0.16	0.95	-0.16	0.96	-0.15	1.15	0.05	0.26	0.03
fbPublicFigures	0.83	0.98	0.16	0.99	0.17	0.96	0.15	0.86	0.17	0.31	0.03
github	2.89	1.2	-0.83	1.03	-0.94	1.67	-0.54	3.34	0.0	0.1	0.13
gowalla	2.5	1.22	-0.69	1.04	-0.83	1.54	-0.48	4.02	0.0	0.05	0.38
internet	1.76	0.93	-0.61	0.75	-0.81	1.49	-0.17	2.03	0.0	0.13	0.13
lastfm	0.59	0.67	0.14	0.72	0.2	0.76	0.26	0.61	0.41	0.35	0.03
liveJournal	1.27	1.35	0.06	1.35	0.06	1.24	-0.03	1.31	0.04	0.19	0.03
livemocha	1.65	1.47	-0.12	1.45	-0.13	1.56	-0.06	1.66	0.02	0.35	0.0
museaFacebook	0.84	0.97	0.14	1.01	0.18	1.02	0.19	0.88	0.22	0.27	0.05
pgp	0.57	0.59	0.03	0.69	0.19	0.68	0.17	0.7	0.28	0.16	0.18
PIN	0.25	0.29	0.13	0.23	-0.09	0.38	0.38	0.26	0.92	0.63	0.01
powergrid	0.18	0.2	0.1	0.2	0.13	0.22	0.24	0.35	1.73	0.09	0.5
roadCA	0.04	0.16	1.21	0.15	1.19	0.16	1.23	5.0	35.48	0.0	0.99
roadPA	0.04	0.15	1.21	0.16	1.21	0.17	1.25	5.0	39.43	0.0	0.99
roadTX	0.04	0.16	1.21	0.15	1.19	0.16	1.23	5.0	36.7	0.0	0.99
twitch	2.76	1.67	-0.49	1.5	-0.59	2.06	-0.29	2.82	0.0	0.21	0.02
wordnet	0.87	0.88	0.02	0.82	-0.06	0.99	0.13	0.89	0.14	0.28	0.02
youtube	1.92	1.27	-0.41	1.09	-0.55	1.71	-0.12	2.39	0.0	0.08	0.2

## 2. Gamma

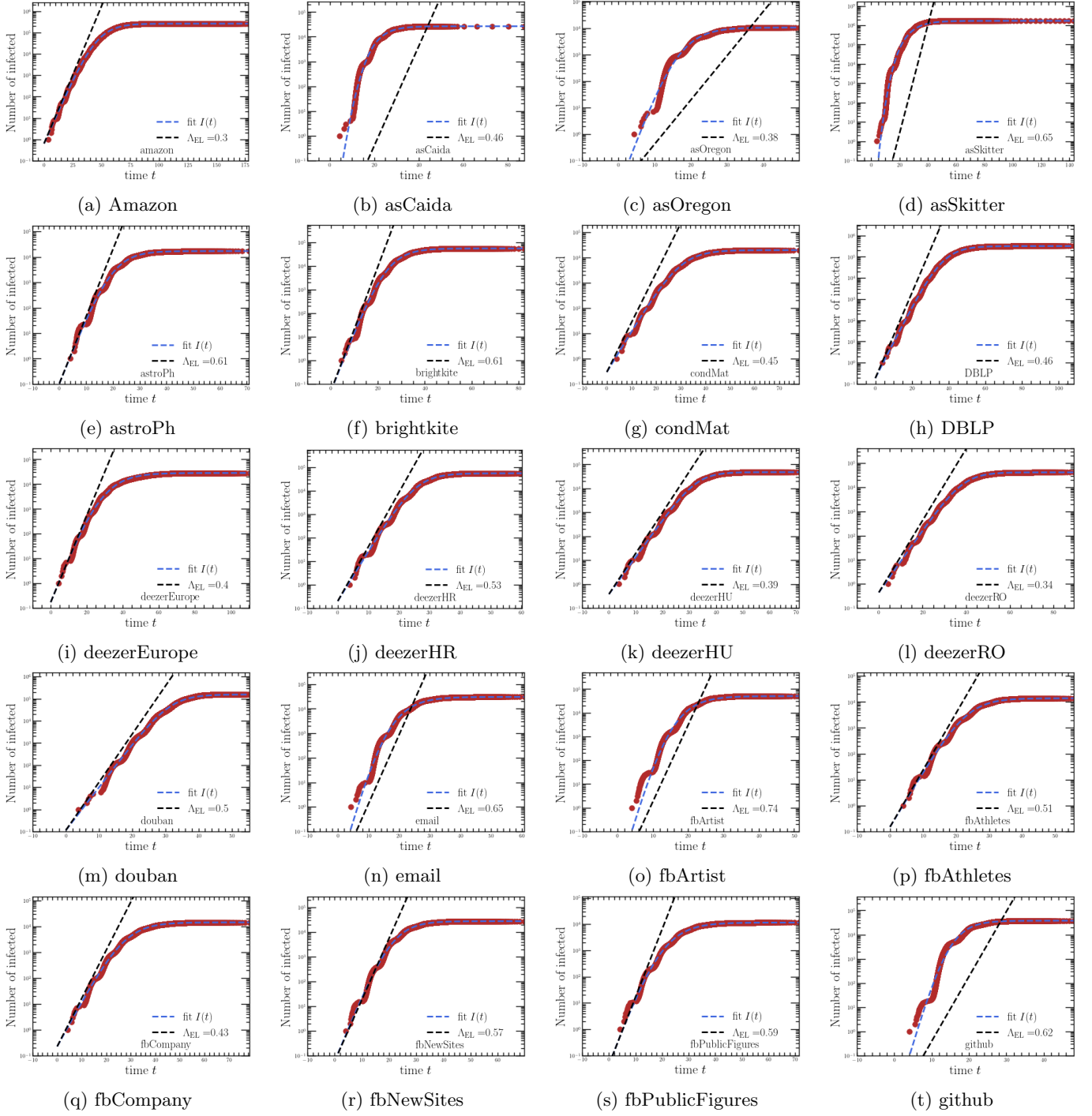


FIG. 20: Average epidemic trajectories on real-world networks with a Gamma generation-time distribution (I).

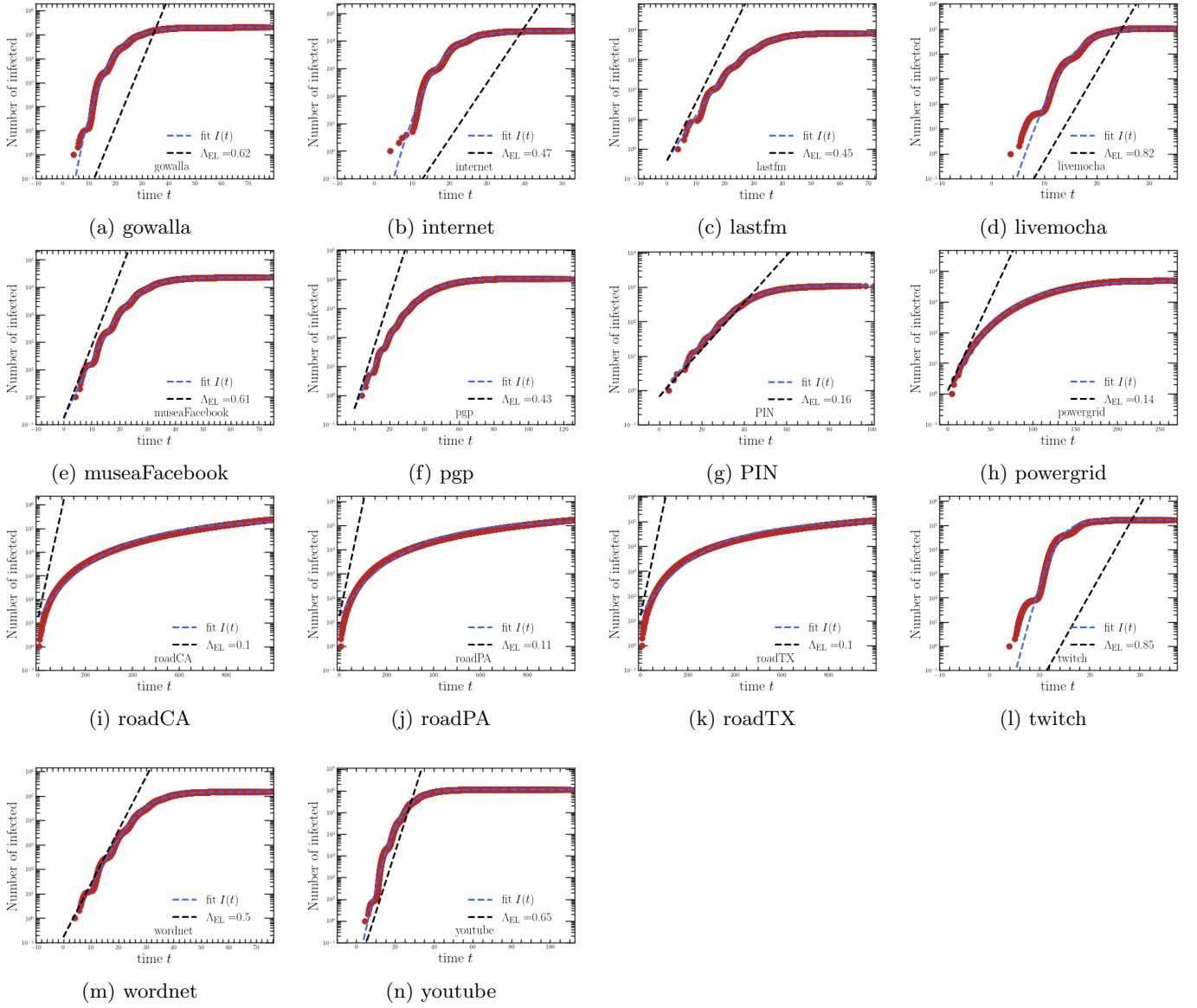


FIG. 21: Average epidemic trajectories on real-world networks with a Gamma generation-time distribution (I).

TABLE VII: Results and parameters from the fitting procedure on real-world networks with a Gamma generation-time distribution.

Network	$\Lambda_{\text{FIT}}$	$\Lambda_R$	Error $_R$	$\Lambda_{R_{\text{pert}}}$	Error $_{R_{\text{pert}}}$	$\Lambda_{R_0}$	Error $_{R_0}$	$\Lambda_0$	$I_{0(\text{fit})}$	$\nu$	$\eta$
amazon	0.28	0.3	0.07	0.3	0.06	0.34	0.19	0.28	0.64	0.36	0.01
asCaida	1.45	0.56	-0.89	0.46	-1.03	0.85	-0.52	1.59	0.0	0.12	0.09
asOregon	0.83	0.51	-0.48	0.38	-0.73	0.84	0.01	0.85	0.01	0.27	0.02
asSkitter	2.31	0.87	-0.9	0.65	-1.12	1.12	-0.69	5.0	0.0	0.02	0.54
astroPh	0.6	0.59	-0.01	0.61	0.02	0.62	0.04	0.61	0.11	0.34	0.02
brightkite	0.58	0.59	0.02	0.61	0.05	0.62	0.06	0.59	0.05	0.31	0.01
condMat	0.37	0.44	0.17	0.45	0.2	0.45	0.19	0.37	0.3	0.47	0.01
DBLP	0.39	0.43	0.09	0.46	0.17	0.45	0.14	0.39	0.19	0.4	0.0
deezerEurope	0.42	0.4	-0.03	0.4	-0.03	0.4	-0.04	0.43	0.17	0.27	0.04
deezerHR	0.49	0.53	0.09	0.53	0.09	0.53	0.08	0.49	0.2	0.49	0.0
deezerHU	0.36	0.39	0.1	0.39	0.09	0.39	0.09	0.36	0.38	0.67	0.0
deezerRO	0.3	0.34	0.14	0.34	0.15	0.34	0.13	0.3	0.44	0.62	0.0
douban	0.45	0.51	0.13	0.5	0.11	0.53	0.17	0.45	0.11	0.56	0.0
email	1.0	0.66	-0.41	0.65	-0.43	0.74	-0.3	1.05	0.0	0.18	0.05
fbArtist	1.16	0.75	-0.43	0.74	-0.44	0.76	-0.42	1.2	0.0	0.19	0.04
fbAthletes	0.49	0.51	0.03	0.51	0.03	0.54	0.09	0.49	0.15	0.46	0.01
fbCompany	0.4	0.43	0.07	0.43	0.07	0.45	0.12	0.4	0.23	0.41	0.01
fbNewSites	0.61	0.57	-0.06	0.57	-0.06	0.58	-0.05	0.62	0.06	0.33	0.01
fbPublicFigures	0.61	0.59	-0.03	0.59	-0.02	0.58	-0.04	0.63	0.04	0.26	0.04
github	1.2	0.7	-0.53	0.62	-0.64	0.93	-0.26	1.22	0.0	0.24	0.01
gowalla	1.7	0.71	-0.82	0.62	-0.93	0.87	-0.65	2.28	0.0	0.06	0.26
internet	1.23	0.56	-0.74	0.47	-0.9	0.84	-0.38	1.32	0.0	0.15	0.07
lastfm	0.35	0.42	0.18	0.45	0.23	0.47	0.28	0.36	0.4	0.41	0.02
livemocha	1.44	0.84	-0.53	0.82	-0.55	0.88	-0.49	1.47	0.0	0.2	0.02
museaFacebook	0.5	0.58	0.15	0.61	0.19	0.61	0.19	0.52	0.17	0.31	0.03
pgp	0.32	0.37	0.15	0.43	0.29	0.42	0.27	0.35	0.34	0.24	0.09
PIN	0.18	0.19	0.07	0.16	-0.14	0.25	0.31	0.18	0.65	0.61	0.01
powergrid	0.13	0.13	-0.0	0.14	0.02	0.15	0.13	0.32	1.27	0.06	0.59
roadCA	0.03	0.11	1.02	0.1	1.0	0.11	1.04	5.0	17.23	0.0	0.99
roadPA	0.04	0.11	0.98	0.11	0.99	0.11	1.03	5.0	17.25	0.0	0.99
roadTX	0.04	0.11	0.99	0.1	0.96	0.11	1.0	5.0	16.23	0.0	0.99
twitch	1.86	0.93	-0.67	0.85	-0.75	1.1	-0.51	1.86	0.0	0.25	0.0
wordnet	0.49	0.54	0.09	0.5	0.02	0.6	0.19	0.5	0.17	0.34	0.01
youtube	0.99	0.74	-0.29	0.65	-0.42	0.94	-0.04	1.06	0.0	0.13	0.07

## 3. Weibull

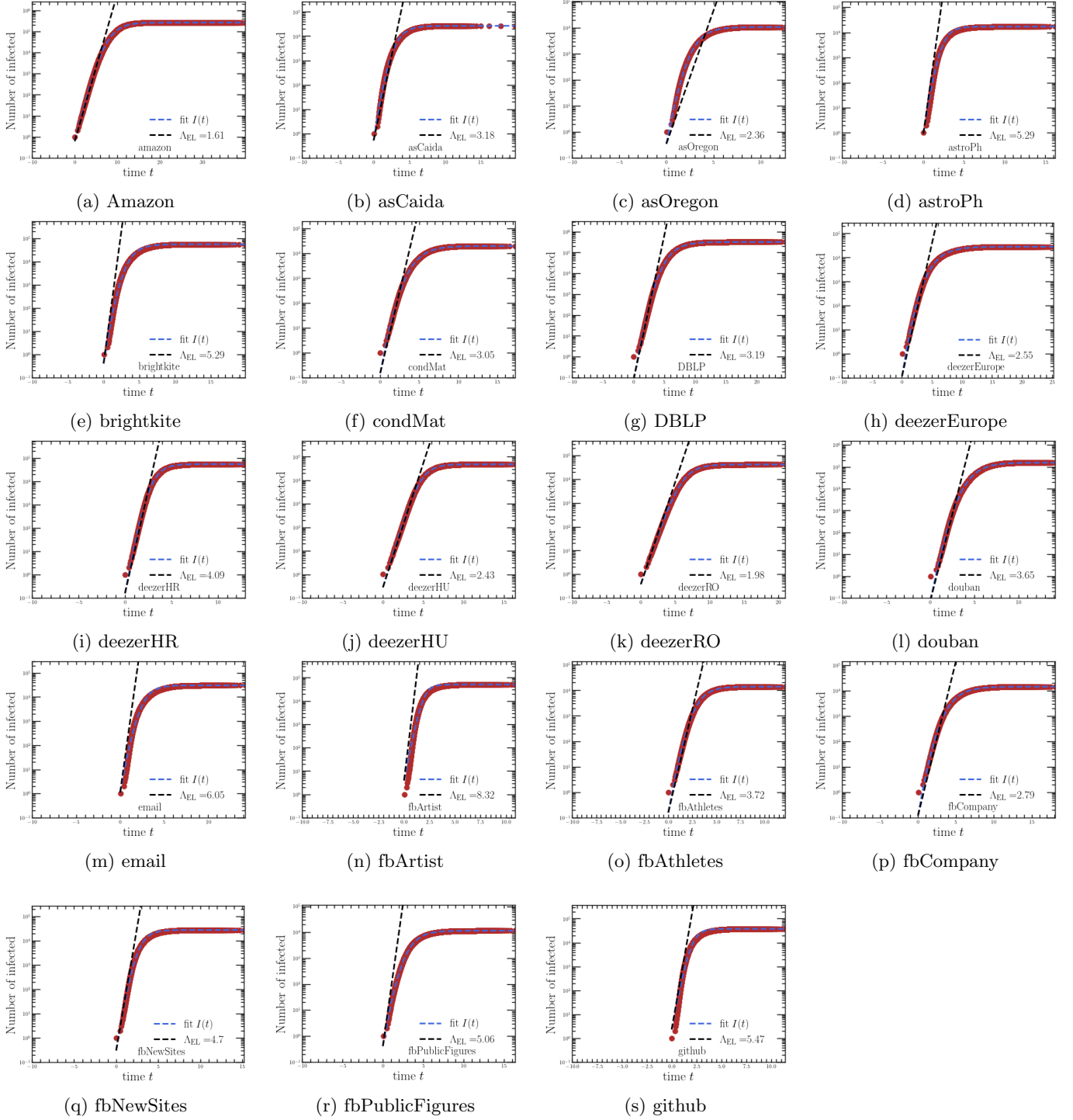


FIG. 22: Average epidemic trajectories on real-world networks with a Weibull generation-time distribution (I).

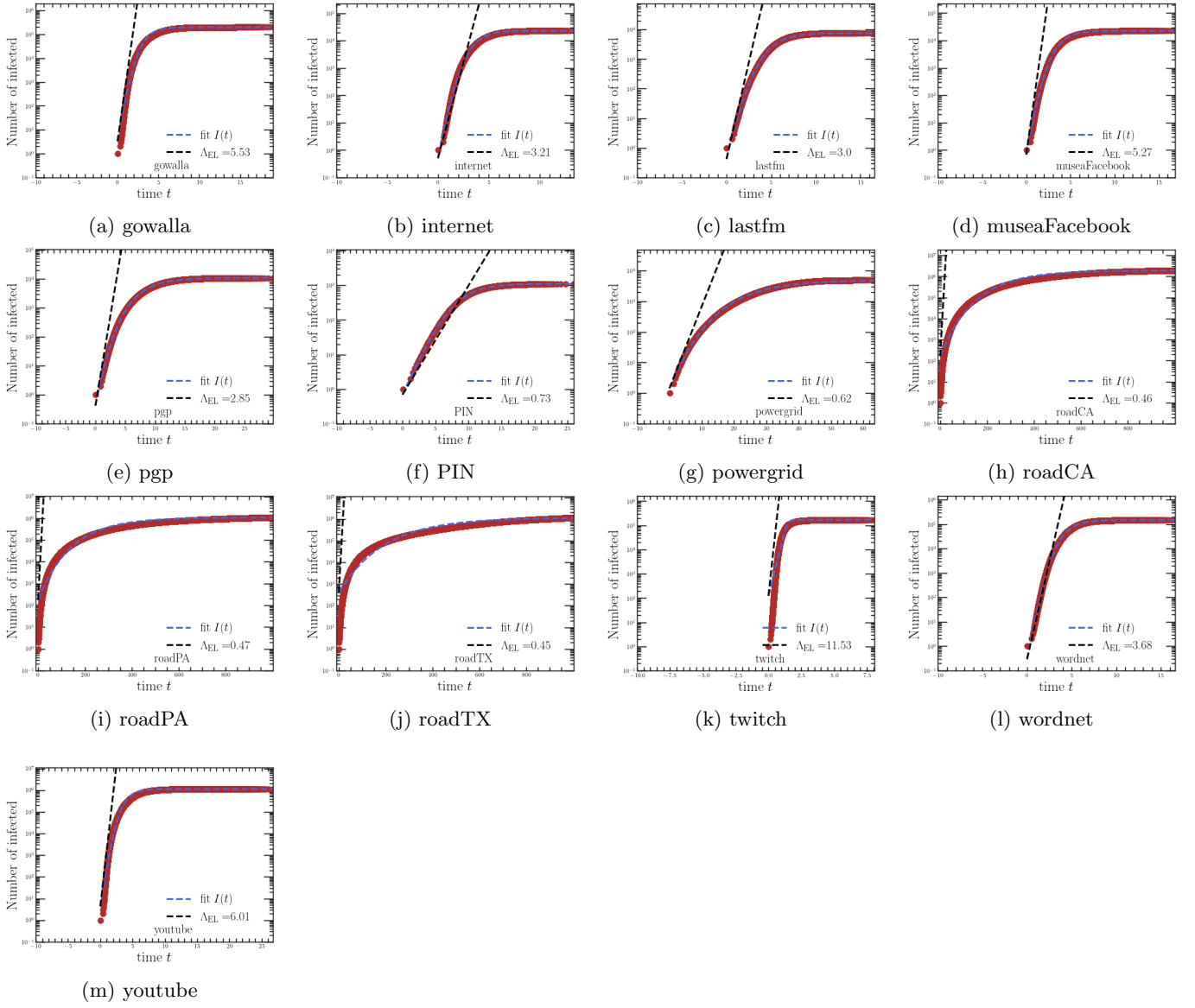


FIG. 23: Average epidemic trajectories on real-world networks with a Weibull generation-time distribution (I).

TABLE VIII: Results and parameters from the fitting procedure on real-world networks with a Weibull generation-time distribution.

Network	$\Lambda_{\text{FIT}}$	$\Lambda_R$	Error $_R$	$\Lambda_{R_{\text{pert}}}$	Error $_{R_{\text{pert}}}$	$\Lambda_{R_0}$	Error $_{R_0}$	$\Lambda_0$	$I_{0(\text{fit})}$	$\nu$	$\eta$
amazon	1.77	1.65	-0.08	1.61	-0.1	1.95	0.09	1.84	0.62	0.26	0.03
asCaida	4.27	4.51	0.06	3.18	-0.29	11.75	0.93	5.0	0.52	0.18	0.15
asOregon	4.21	3.77	-0.11	2.36	-0.57	11.14	0.9	5.0	0.35	0.18	0.16
asSkitter	4.8	12.43	0.89	6.02	0.23	26.84	1.39	5.0	14.54	0.27	0.04
astroPh	4.58	4.98	0.08	5.29	0.14	5.54	0.19	5.0	0.92	0.25	0.08
brightkite	4.3	5.03	0.15	5.29	0.21	5.47	0.24	5.0	0.41	0.17	0.14
condMat	3.74	2.91	-0.25	3.05	-0.2	3.03	-0.21	4.64	0.15	0.14	0.19
DBLP	3.64	2.79	-0.26	3.19	-0.13	3.0	-0.19	4.08	0.08	0.15	0.11
deezerEurope	3.52	2.53	-0.33	2.55	-0.32	2.5	-0.34	5.0	0.12	0.1	0.3
deezerHR	4.77	4.08	-0.16	4.09	-0.15	4.0	-0.17	5.0	0.16	0.24	0.05
deezerHU	2.62	2.44	-0.07	2.43	-0.07	2.4	-0.08	2.64	0.28	0.38	0.01
deezerRO	1.95	1.96	0.01	1.98	0.02	1.94	-0.0	1.97	0.38	0.38	0.01
douban	4.4	3.82	-0.14	3.65	-0.19	4.07	-0.08	5.0	0.08	0.15	0.12
email	4.5	6.35	0.34	6.05	0.29	8.25	0.59	5.0	1.1	0.23	0.1
fbArtist	4.93	8.35	0.51	8.32	0.51	8.74	0.56	5.0	3.91	0.46	0.01
fbAthletes	4.55	3.72	-0.2	3.72	-0.2	4.16	-0.09	5.0	0.16	0.21	0.09
fbCompany	3.86	2.77	-0.33	2.79	-0.32	3.02	-0.24	5.0	0.12	0.13	0.23
fbNewSites	4.67	4.72	0.01	4.7	0.01	4.83	0.03	5.0	0.3	0.24	0.07
fbPublicFigures	4.05	4.93	0.2	5.06	0.22	4.84	0.18	5.0	0.41	0.16	0.19
github	4.87	7.21	0.39	5.47	0.12	14.78	1.01	5.0	2.31	0.37	0.03
gowalla	4.43	7.49	0.51	5.53	0.22	12.3	0.94	5.0	3.27	0.2	0.11
internet	4.29	4.58	0.07	3.21	-0.29	11.35	0.9	5.0	0.51	0.18	0.14
lastfm	2.82	2.74	-0.03	3.0	0.06	3.29	0.15	3.4	0.42	0.18	0.17
livemocha	5.0	11.14	0.76	10.74	0.73	12.72	0.87	5.0	15.26	0.82	0.0
museaFacebook	4.09	4.87	0.17	5.27	0.25	5.35	0.27	5.0	0.68	0.16	0.18
pgp	2.4	2.26	-0.06	2.85	0.17	2.75	0.14	5.0	0.42	0.06	0.52
PIN	0.95	0.94	-0.02	0.73	-0.27	1.27	0.28	1.01	0.69	0.4	0.05
powergrid	0.59	0.6	0.02	0.62	0.05	0.7	0.17	1.67	1.43	0.05	0.65
roadCA	0.06	0.47	1.52	0.46	1.51	0.49	1.53	5.0	161.13	0.0	0.99
roadPA	0.06	0.46	1.53	0.47	1.53	0.5	1.56	5.0	175.98	0.0	0.99
roadTX	0.04	0.47	1.68	0.45	1.66	0.48	1.68	5.0	392.36	0.0	0.99
twitch	5.0	14.8	0.99	11.53	0.79	25.47	1.34	5.0	122.42	1.56	0.0
wordnet	4.42	4.18	-0.06	3.68	-0.18	5.08	0.14	5.0	0.29	0.16	0.12
youtube	4.44	8.12	0.59	6.01	0.3	15.66	1.12	5.0	4.37	0.17	0.11

### G. Comparison between estimates of the reproduction number

It is possible, in principle, to use  $R_0$  instead of  $R_{\text{pert}}$  to predict the spreading rate by means of the network Euler-Lotka equation. We here test the performance of this simpler approach.

For synthetic networks, the predictions of  $\Lambda$  by the network Euler-Lotka equation using  $R_{\text{pert}}$  as the reproduction number are very accurate (Fig. 24a). In contrast, using  $R_0$  leads to an overestimate of the spreading rates (Fig. 24b). The reason is that  $R_0$  tends to over-estimate the reproduction number (see Table 1 in the Main Text), most noticeably for Barabási-Albert and Watts–Strogatz networks. The relative errors on  $\Lambda$  using  $R_{\text{pert}}$  and  $R_0$  for different synthetic networks and generation time distributions are listed in Tables III, IV, and V.

For real-world networks, the predictions of  $\Lambda$  using  $R_{\text{pert}}$  are more accurate on average than those using  $R_0$ , as long as  $\eta < 0.5$  (see Fig. 25a). For larger values of  $\eta$ ,  $R_0$  provides slightly more accurate predictions of the spreading rate (Fig. 25a), although  $R_{\text{pert}}$  still provides a better estimate of the reproduction number (Fig. 25b). As discussed in the Main Text, this suggests a compensatory effect acting for large  $\eta$ . Examples of comparison between the exponential spreading rates estimated using  $R_{\text{pert}}$  and  $R_0$  are shown in Fig. 26

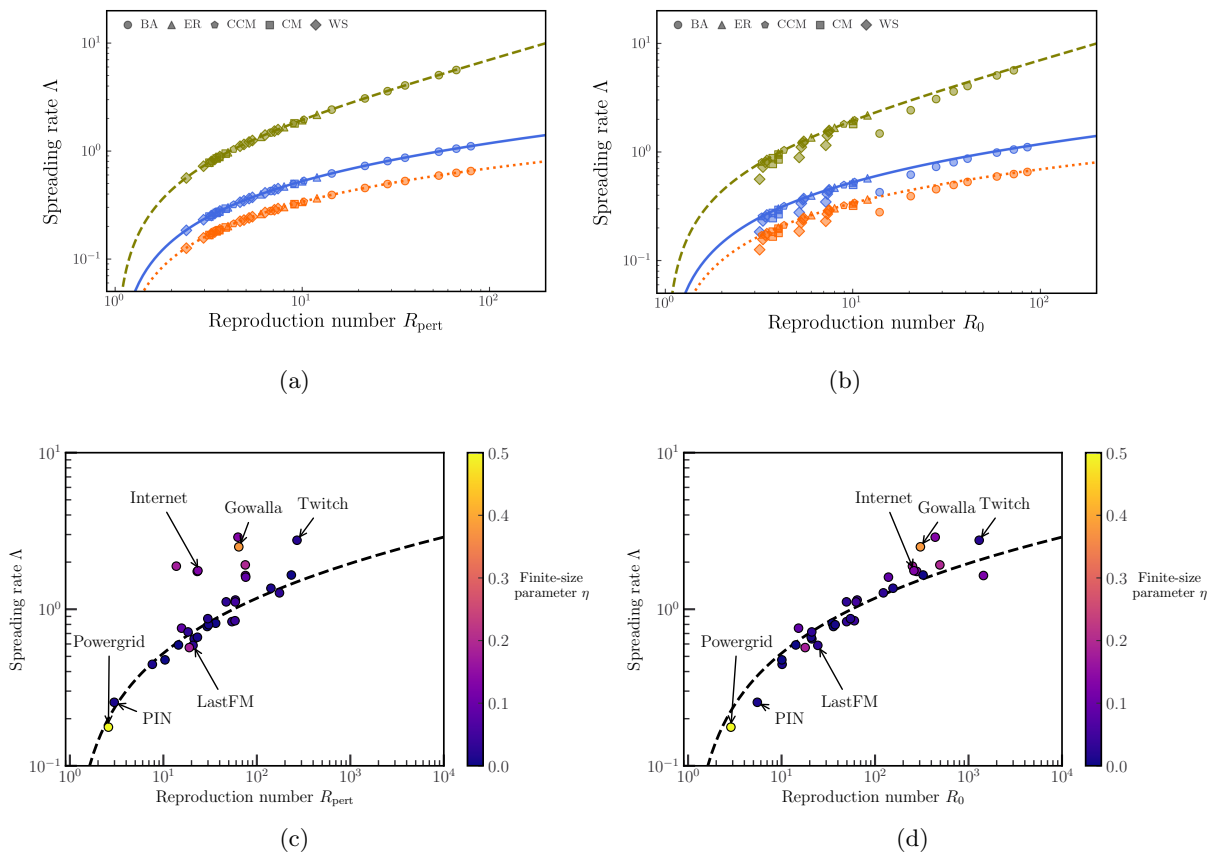


FIG. 24: Comparison of the prediction of the spreading rate using different estimates of the reproduction number. (a) Same as Fig. 2c in the Main Text. (b) Same as Fig. 2c in the Main Text, but using  $R_0$  instead of  $R_{\text{pert}}$ . (c) Same as Fig. 3c in the Main Text. (d) Same as Fig. 3c in the Main Text, but using  $R_0$  instead of  $R_{\text{pert}}$ .

### VI. ESTIMATING THE TAIL OF THE DEGREE DISTRIBUTION

We say that a degree distribution follows a pure power law if it is of the form

$$P(k) = ck^{-\gamma}, \quad c > 0, \gamma > 0. \quad (67)$$

However, real-world data are often better fit by other distributions [14], such as a lognormal. Not even the degree distribution of the Barabási-Albert model follows a pure power law [9], although it is considered as the emblematic

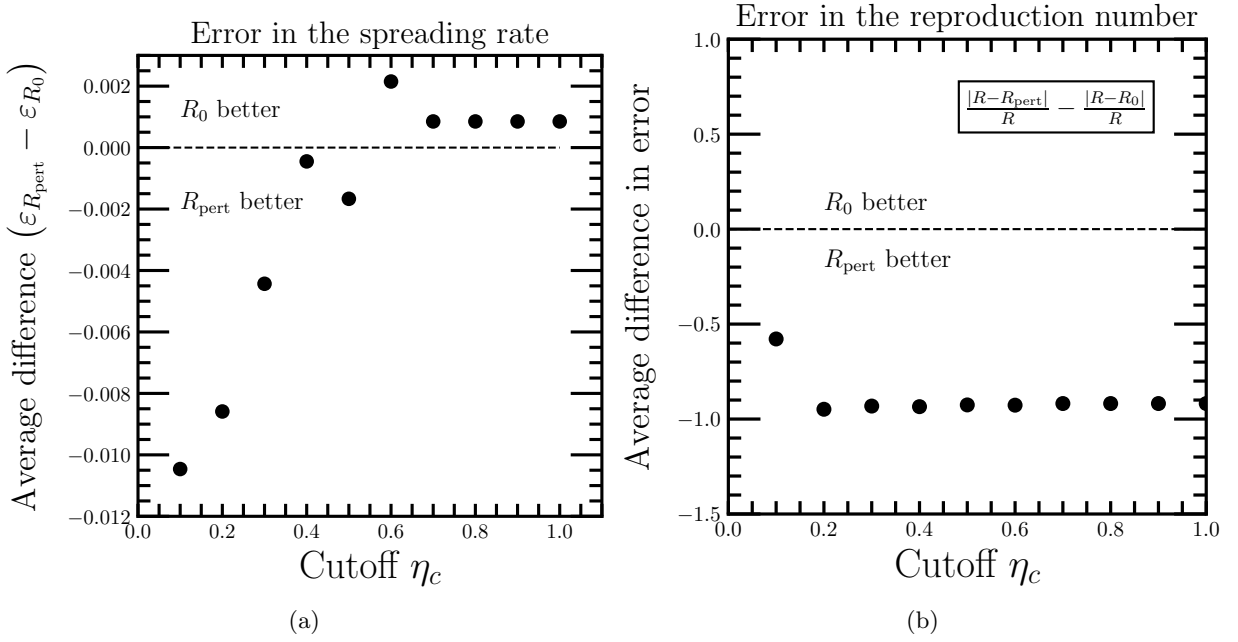


FIG. 25: **Performance of  $R_{\text{pert}}$  and  $R_0$  for different values of the finite-size parameter  $\eta$ .** (a). Mean difference between the relative errors of spreading rates estimated using  $R_{\text{pert}}$  and  $R_0$  as a function of the finite-size parameter  $\eta$ . Each dot represents the average of  $\varepsilon_{R_{\text{pert}}} - \varepsilon_{R_0} = 2|\Lambda_{R_{\text{pert}}} - \Lambda_{\text{fit}}|/(\Lambda_{R_{\text{pert}}} + \Lambda_{\text{fit}}) - 2|\Lambda_{R_0} - \Lambda_{\text{fit}}|/(\Lambda_{R_0} + \Lambda_{\text{fit}})$  across all cases where  $\eta \leq \eta_c$ . (b). Mean difference between the errors of  $R_{\text{pert}}$  and  $R_0$  as estimators of the reproduction number  $R$  is a function of the finite-size parameter  $\eta_c$ . Each dot represents the average of  $|R_{\text{pert}} - R|/R - |R_0 - R|/R$  across all cases where  $\eta \leq \eta_c$ .

model of power-law degree distributions.

We say that a degree distribution is heavy-tailed if it can be expressed in the form:

$$P(k) = \ell(k)k^{-\gamma}, \quad (68)$$

where  $f(k)$  is a slowly varying function, i.e. a function which satisfies

$$\lim_{k \rightarrow \infty} \frac{f(xk)}{f(k)} = 1. \quad (69)$$

This definition generalises the concept of scale-free networks beyond pure power-law degree distributions. Our goal is to determine the exponent  $\gamma$  when the degree distribution has the form of Eq. (68). We follow the method in [15]. Rather than directly estimating  $\gamma$ , the method estimates the parameter  $\xi = (\gamma - 1)^{-1}$ , which can be interpreted as an extreme value index. When  $\xi > 0$ ,  $P(k)$  is a heavy-tailed distribution and its exponent  $\gamma$  is given by  $\gamma = 1 + 1/\xi$ . There exist various methods to estimate  $\xi$  in a consistent way [15]. From a public software [16], we use the kernel estimator [17], which we observed to capture well the tail of the degree distribution. When the kernel method fails, we use the method of moments. We provide the values of  $\gamma$  estimated with different methods for all real networks in Table IX.

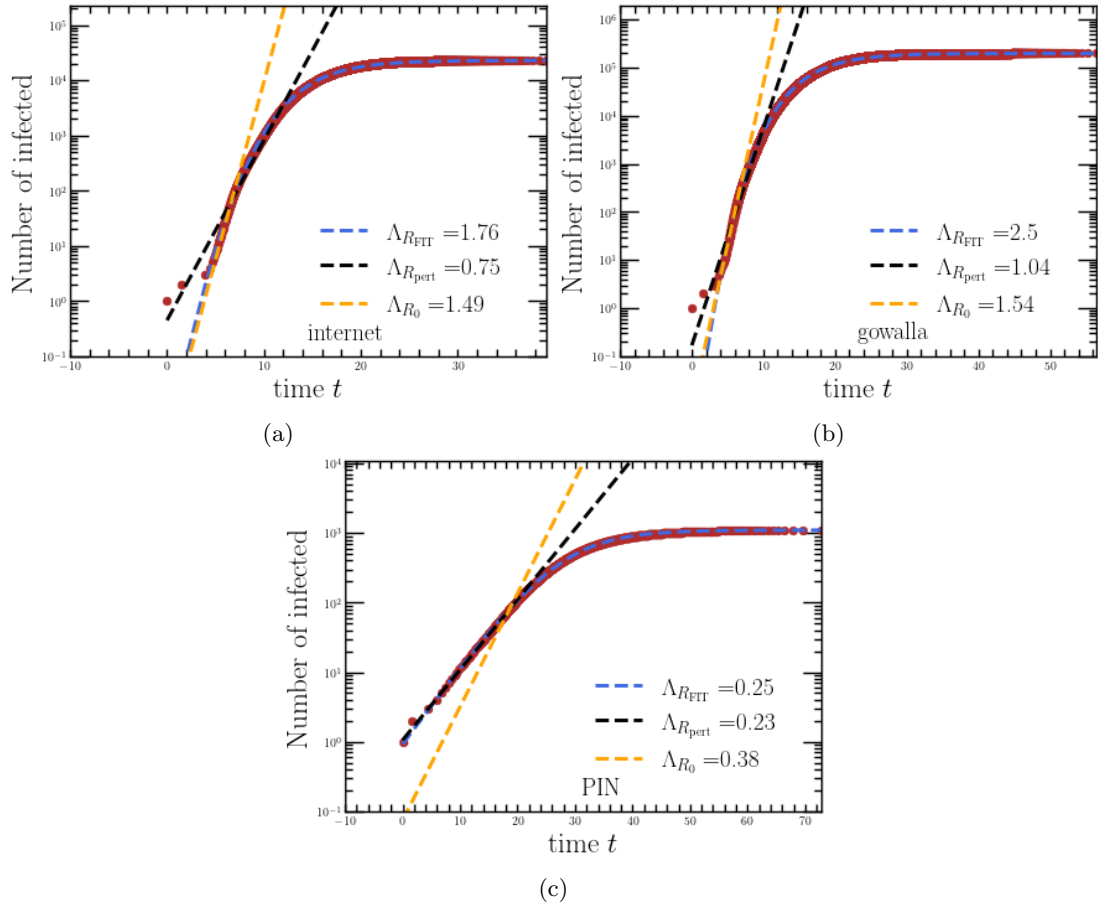


FIG. 26: **Illustration of the difference between  $R_{pert}$  and  $R_0$  for various networks.** We simulate the average epidemic using a lognormal distribution on four different networks: internet (a), gowalla (b) and PIN (c). We compare the difference in the spreading rates using different estimates of the reproduction number. The first two networks do not exhibit a clear exponential regime (internet:  $\eta = 0.13$ , Gowalla:  $\eta = 0.38$ , opposed to PIN:  $\eta = 0.01$ )

TABLE IX: Exponent of the tail of the degree distribution for real networks.

Network	$\gamma_{\text{hill}}$	$\gamma_{\text{moments}}$	$\gamma_{\text{kernel}}$
amazon	3.68	3.43	3.71
asCaida	2.12	2.11	2.13
asOregon	2.07	2.12	2.12
asSkitter	2.38	2.36	2.44
astroPh	4.46	5.68	7.36
brightkite	3.50	3.80	2.96
condMat	3.66	4.09	4.01
DBLP	6.54	14.89	3.09
deezerEurope	4.91	5.01	5.56
deezerHR	4.67	22.17	5.93
deezerHU	5.43	-89.82	7.63
deezerRO	4.98	8.13	5.46
douban	4.40	9.39	7.11
email	12.58	3.38	2.13
fbArtist	3.15	3.18	3.05
fbAthletes	3.24	3.71	56.00
fbCompany	3.51	3.76	4.00
fbNewSites	3.27	3.70	81.76
fbPublicFigures	9.50	-2.03	3.03
github	2.55	2.53	2.56
gowalla	2.81	2.79	2.86
internet	2.08	2.10	2.10
lastfm	3.76	3.90	3.57
liveJournal	3.60	4.09	3.31
livemocha	7.04	-5.77	2.38
museaFacebook	3.35	3.71	3.85
pgp	4.11	4.40	4.48
PIN	3.12	3.53	3.61
powergrid	7.44	7.63	9.14
roadCA	18.79	-1.56	3.27
roadPA	18.30	-1.65	3.35
roadTX	21.66	-1.42	7.16
twitch	2.54	2.56	2.67
wordnet	28.76	2.67	2.60
youtube	2.48	2.58	2.17

TABLE X: Comparison of  $\gamma$  values for different networks

- 
- [1] Cohen, R., Erez, K., Ben-Avraham, D. & Havlin, S. Resilience of the internet to random breakdowns. *Physical Review Letters* **85**, 4626 (2000).
- [2] Newman, M. E. Spread of epidemic disease on networks. *Physical Review E* **66**, 016128 (2002).
- [3] Noh, J. D. Percolation transition in networks with degree-degree correlation. *Physical Review E* **76**, 026116 (2007).
- [4] Newman, M. E. Assortative mixing in networks. *Physical Review Letters* **89**, 208701 (2002).
- [5] Serrano, M. Á. & Boguna, M. Clustering in complex networks. I. General formalism. *Physical Review E* **74**, 056114 (2006).
- [6] Serrano, M. A. & Boguná, M. Tuning clustering in random networks with arbitrary degree distributions. *Physical Review E* **72**, 036133 (2005).
- [7] Pigolotti, S. Generalized Euler-Lotka equation for correlated cell divisions. *Physical Review E* **103**, L060402 (2021).
- [8] Glynn, P. W. & Whitt, W. Large deviations behavior of counting processes and their inverses. *Queueing Systems* **17**, 107–128 (1994).
- [9] Pósfai, M. & Barabási, A.-L. *Network Science* (Citeseer, 2016).
- [10] Leskovec, J. & Krevl, A. SNAP Datasets: Stanford large network dataset collection. <http://snap.stanford.edu/data> (2014).
- [11] Clauset, A., Tucker, E. & Sainz, M. The Colorado Index of Complex Networks. <https://icon.colorado.edu/> (2016).
- [12] Kunegis, J. KONECT – The Koblenz Network Collection. In *Proc. Int. Conf. on World Wide Web Companion*, 1343–1350 (2013). URL <http://dl.acm.org/citation.cfm?id=2488173>.

- [13] Gibson, M. A. & Bruck, J. Efficient exact stochastic simulation of chemical systems with many species and many channels. *The journal of physical chemistry A* **104**, 1876–1889 (2000).
- [14] Broido, A. D. & Clauset, A. Scale-free networks are rare. *Nature Communications* **10**, 1017 (2019).
- [15] Voitalov, I., Van Der Hoorn, P., Van Der Hofstad, R. & Krioukov, D. Scale-free networks well done. *Physical Review Research* **1**, 033034 (2019).
- [16] Voitalov, I. Tail index estimation for degree sequences of complex networks. <https://github.com/ivanvoitalov/tail-estimation> (2018).
- [17] Groeneboom, P., Lopuhaä, H. P. & De Wolf, P. Kernel-type estimators for the extreme value index. *The Annals of Statistics* **31**, 1956–1995 (2003).